© 2017. Published by The Company of Biologists Ltd | Development (2017) 144, 2415-2427 doi:10.1242/dev.149641

RESEARCH ARTICLE

The matrix protein Tiggrin regulates plasmatocyte maturation in *Drosophila* larva

Chen U. Zhang and Ken M. Cadigan*

ABSTRACT

The lymph gland (LG) is a major source of hematopoiesis during *Drosophila* development. In this tissue, prohemocytes differentiate into multiple lineages, including macrophage-like plasmatocytes, which comprise the vast majority of mature hemocytes. Previous studies have uncovered genetic pathways that regulate prohemocyte maintenance and some cell fate choices between hemocyte lineages. However, less is known about how the plasmatocyte pool of the LG is established and matures. Here, we report that Tiggrin, a matrix protein expressed in the LG, is a specific regulator of plasmatocyte maturation. *Tiggrin* mutants exhibit precocious maturation of plasmatocytes, whereas Tiggrin overexpression blocks this process, resulting in a buildup of intermediate progenitors (IPs) expressing prohemocyte and hemocyte markers. These IPs likely represent a transitory state in prohemocyte to plasmatocyte differentiation. We also found that overexpression of Wee1 kinase, which slows G_2/M progression, results in a phenotype similar to Tiggrin overexpression, whereas String/Cdc25 expression phenocopies *Tiggrin* mutants. Further analysis revealed that Wee1 inhibits plasmatocyte maturation through upregulation of *Tiggrin* transcription. Our results elucidate connections between the extracellular matrix and cell cycle regulators in the regulation of hematopoiesis.

KEY WORDS: *Drosophila* lymph gland, Hematopoiesis, Plasmatocyte, Tiggrin, Cell cycle

INTRODUCTION

In *Drosophila*, hemocytes are initially specified from the procephalic mesoderm and undergo further amplification during larval development (Lebestky et al., 2000; Makhijani et al., 2011; Markus et al., 2009). In parallel, precursor cells of the lymph gland (LG) assemble in the dorsal thoracic mesoderm during embryogenesis and develop during larval stages into several pairs of lobes aligned on the dorsal vessel (Holz et al., 2003; Jung et al., 2005). The cells of this tissue undergo hematopoiesis, and the LG dissembles at the start of pupation, releasing mature hemocytes into circulation, where they assist with tissue remodeling during metamorphosis (Grigorian et al., 2011; Lanot et al., 2001).

During the 3rd instar stage, the LG contains two disk-shaped primary lobes (PLs) that typically contain a few thousand cells divided into three domains. A centrally located medullary zone (MZ) contains prohemocytes with stem cell-like properties, whereas differentiating hemocytes are located in the peripheral cortical zone (CZ) (Evans et al., 2009; Jung et al., 2005). In addition, a small group of cells termed the posterior signaling center (PSC) controls differentiation and specification of hemocytes in the CZ (Benmimoun et al., 2015; Oyallon et al., 2016). Although much remains to be understood, the fly LG has developed into a powerful model for hematopoiesis and stem cell/progenitor regulation (Crozatier and Meister, 2007; Crozatier and Vincent, 2011; Letourneau et al., 2016; Martinez-Agosto et al., 2007; Morin-Poulard et al., 2013; Shim et al., 2013).

There are three major lineages of mature hemocytes in *Drosophila*: plasmatocytes, crystal cells and lamellocytes, all of which can be produced by the LG. Plasmatocytes contribute about 95% of all mature hemocytes in healthy animals (Crozatier and Meister, 2007; Letourneau et al., 2016). These cells are the equivalent of mammalian macrophages, which are able to clean both apoptotic debris and foreign materials (Gold and Brückner, 2015). They also play important roles in innate immunity (Charroux and Royet, 2009; Gold and Brückner, 2015) and participate in tissue regeneration by activating stem cells near sites of injury (Ayyaz et al., 2015). Crystal cells are specialized non-phagocytic cells that facilitate immune responses and wound-healing by causing melanization (Lanot et al., 2001). Lamellocytes are rarely found in healthy animals, but their number is significantly increased when larvae are immunologically challenged with infection by a parasitic wasp (Crozatier et al., 2004; Honti et al., 2014; Rizki and Rizki, 1992).

The genetic control of cell fate in the PL has been extensively studied, and several signaling pathways are known to be important for its proper development. For example, the Wnt protein Wingless (Wg) is expressed in the MZ, where it promotes prohemocyte proliferation and maintenance (Sinenko et al., 2009). Notch signaling controls the crystal cell-lamellocyte decision, as inhibition of this pathway resulted in a reduction in crystal cells and a large increase in lamellocytes in healthy larvae (Duvic et al., 2002; Small et al., 2014). Crystal cell number in the PL is also controlled by Hippo signaling, which restricts specification of this cell type (Ferguson and Martinez-Agosto, 2014; Milton et al., 2014). By comparison with crystal cells and lamellocytes, the maturation process of the largest hemocyte population in the LG, the plasmatocytes, remains relatively obscure.

The working model of the larval LG states that plasmatocytes are derived from prohemocytes. Consistent with this, a population of cells that expresses both MZ and CZ markers has been observed in the PL (Dragojlovic-Munther and Martinez-Agosto, 2012; Sinenko et al., 2009), as well as cells that possess CZ markers but lack mature plasmatocyte markers (Minakhina et al., 2011) or lack both MZ and mature plasmatocyte markers (Krzemien et al., 2010). These intermediate progenitors (IPs) are typically found near the MZ and have a higher mitotic capacity than differentiated plasmatocytes (Krzemien et al., 2010). There are some reports of factors

Department of Molecular, Cellular and Developmental Biology, University of Michigan, Ann Arbor, MI 48109, USA.

*Author for correspondence (cadigan@umich.edu)

K.M.C., 0000-0003-2431-1703

Received 29 January 2017; Accepted 11 May 2017

Development (2017) 144, 2415-2427 doi:10.1242/dev.149641

controlling this IP pool, e.g. the transcription factor Pannier (Minakhina et al., 2011), but it has been difficult to pin down their roles, owing to the transitory nature of this population. The ability to 'lock' cells in this intermediate stage would be an important tool for better understanding their role in LG hematopoiesis.

We have previously reported that Wg signaling represses the expression of *Tiggrin* (*Tig*) in embryonic hemocytes and in the PL of the LG (Blauwkamp et al., 2008; Zhang et al., 2014). *Tig* encodes a large extracellular matrix (ECM) protein that binds to integrins and is important for muscle attachment and cell-cell adhesion (Bunch et al., 1998; Fogerty et al., 1994; Graner et al., 1998; Zhang et al., 2010). The repression of *Tig* transcription by Wg signaling is noteworthy, as it occurs through a direct mechanism involving novel binding sites for the transcription factor TCF/Pangolin (TCF/Pan), which mediates Wg target gene regulation in flies (Zhang et al., 2014). However, the physiological role of this regulation is not clear.

Here, we report on the biological role of Tig in the larval LG, using a combination of loss- and gain-of-function approaches. We found that *Tig* mutants displayed a premature appearance of mature plasmatocytes. Conversely, overexpression of Tig blocked plasmatocyte differentiation, and caused a large buildup of IPs that express both MZ and CZ markers. These manipulations of Tig levels had little or no effect on the number of crystal cells and lamellocytes. Expression of a *Tig* mutant transgene lacking an integrin-binding domain had the same effect as wild-type Tig, suggesting that the function of Tig in the CZ is independent of integrin signaling. In addition, we found that regulators of G_2/M transition dramatically affect plasmatocyte differentiation and likely do so through regulation of Tig expression. These results highlight the connection between cell cycle regulators and the ECM protein Tig in the regulation of hematopoiesis in the fly LG.

RESULTS

Tig is required for maintaining the hemocyte population in the PL of the LG

Tig is an essential gene, with mutants dying as pupae owing to defects in muscle attachment, morphology and function (Bunch et al., 1998). Tig is secreted at muscle attachment sites by circulating hemocytes (Bunch et al., 1998; Fogerty et al., 1994). In addition to its expression in circulating hemocytes, we previously reported that Tig protein and two reporters containing *Tig* cis-regulatory sequences are primarily expressed in the CZ of the PL (Zhang et al., 2014). To examine the role of Tig in the larval LG, we examined PLs in a *Tig* mutant transheterozygous background (Tig^X/Tig^{A1}). The Tig^X allele is a small deletion removing the entire *Tig* locus and parts of two adjacent genes, whereas the Tig^{A1} allele is an EMS-induced point mutation that fails to complement the muscle phenotype of Tig^X (Bunch et al., 1998). *Tig* mutants displayed a dramatic reduction in PL size in late 3rd instars (Fig. 1A,B). Both the CZ and MZ are reduced in *Tig* mutants compared with wild type (Fig. 1C), but the PSC cell number is unaffected (Fig. 1D). These results revealed a previously unexpected role for Tig in the larval LG development.

To confirm the specificity of the *Tig* PL phenotype, a rescue was performed with a P[UAS-Tig] transgene via *Hml*-Gal4, which is active in the CZ of the PL, as well as resident and circulating hemocytes (Goto et al., 2003; Makhijani et al., 2011). In an otherwise wild-type background, Hml>Tig animals displayed no detectable difference in PL size, but Hml>Tig rescued the reduced PL phenotype of Tig^X/Tig^{A1} larvae (Fig. 1E), indicating that the *Tig* mutant PL phenotype was due to loss of *Tig* activity. These data suggest that Tig acts in the CZ to maintain the size of the PL, with the MZ size reduction likely a secondary effect.

Tig^X/Tig^{A1} mutant larvae are more slender and elongated than controls (Bunch et al., 1998), raising the possibility that the reduced PL size is a non-specific effect. To address this, the size of wing and eye-antennal imaginal discs in *Tig* mutants was examined. These tissues were 18-22% smaller in *Tig* mutants than in controls (Fig. S1). Although these reductions are statistically significant, they are less severe than the approximate twofold reduction observed in the PL (Fig. 1C).

To address whether premature release of hemocytes from *Tig* mutants could account for the small PL size, we examined control

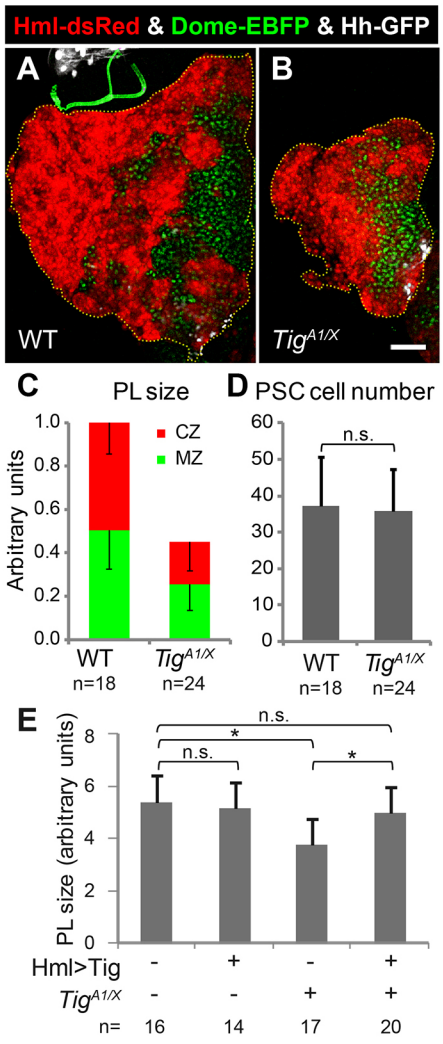

Fig. 1. Tig is important for development of the PL of the LG. (A,B) Confocal images of PLs from mid/late 3rd instar larvae from w^{1118} or $Tig^{A1/X}$ mutant transheterozygotes. The CZ, MZ and PSC are marked by Hml-dsRed (red), Dome-EBFP (green) and Hh-GFP (white), respectively. *Tig* mutants had smaller PLs with less CZ and MZ but unchanged PSC. (C) Quantification shows that the sizes of CZ, MZ and the total PL are significantly different between wild type and *Tig* mutants ($P<0.01$ for all comparisons). (D) No detectable change in PSC cell number is observed in *Tig* mutants. (E) Size of PLs from mid/late 3rd instar larvae containing P[Hml-Gal4] with or without P[UAS-Tig] and *Tig* mutant alleles. Hml>Tig has no effect on PL size by itself but rescued the PL size reduction of *Tig* mutants. The reduction of PL size in *Tig* mutants was less dramatic in the rescue experiment than in C (see also Tables S1 and S2). This is likely due to differences in the genetic backgrounds (i.e. the inclusion of P[Hml-Gal4], P[UAS-GFP] in the rescue data). *$P<0.05$, n.s., not significant. Data are mean±s.e.m. Scale bar: 50 µm.

Development (2017) 144, 2415-2427 doi:10.1242/dev.149641

and *Tig* mutant PLs containing a Vkg>GFP gene trap, which indicates the location of collagen IV in the basal lamina (Morin et al., 2001). Although one-quarter of wild-type PLs have regions that are Vkg^{+} but devoid of cells (suggesting release of hemocytes from that area), the frequency of occurrence was similar in *Tig*^{X}/*Tig*^{A1} mutants (Fig. S2). Early release of LG hemocytes should increase the number of circulating hemocytes in mid/late 3rd instar larvae, but we observed a reduction in *Tig* mutants (Fig. S2). This could be due to a reduction in embryonic hematopoiesis, given the expression of Tig in hemocytes at that stage (Fogerty et al., 1994; Alfonso and Jones, 2002; Blauwkamp et al., 2008). These data revealed no evidence for early release of hemocytes from *Tig* mutant LGs.

Examination of earlier stages revealed that *Tig* mutant PL size was similar to controls at late 2nd larval instar, but were significantly reduced by the early 3rd instar stage (Fig. 2A-G,I; Table S1). A similar trend is observed in CZ size (Fig. 2G,I; Table S1). The difference in PL size between controls and *Tig* mutants was similar whether ascertained using optical slices or volumetrically measured with stacked projections (Table S2). These data indicate a defect in PL and CZ growth starting at the early 3rd larval instar.

Tig mutants display precocious plasmatocyte differentiation

Plasmatocytes are specified throughout the 3rd larval instar stage and constitute the major type of hemocyte in the CZ (Crozatier and Meister, 2007). Plasmatocyte differentiation was monitored with the P1 antibody, which recognizes Nimrod C1 (NimC1), a phagocytosis receptor expressed in mature plasmatocytes (Kurucz et al., 2007). At late 2nd instar, both control and *Tig*^{X}/*Tig*^{A1} PLs had similar low numbers of P1^{+} cells. By early 3rd instar, *Tig* mutants had a significant increase in plasmatocytes compared with wild type, which increased at mid/late 3rd instar (Fig. 2A′-F′,H,I; Table S1). This increase was observed when quantification was performed on optical slices or volumetrically (Table S2). In addition, the 2° lobes of *Tig*^{X}/*Tig*^{A1} LGs had a dramatic increase in plasmatocytes in mid 3rd instars (Fig. 2J,K). Cells in control 2° lobes were small and compact, resembling the MZ of the PL. In contrast, most 2° lobes in *Tig* mutants had larger more loosely packed cells, reminiscent of CZ (Fig. 2L,M; Table S3). Development to pupation occurred slightly later in *Tig* mutants than in controls (Fig. S3), indicating that the precocious appearance of plasmatocytes in *Tig* mutants cannot be explained by a faster developmental clock. These data indicate that Tig suppresses plasmatocyte maturation in the LG.

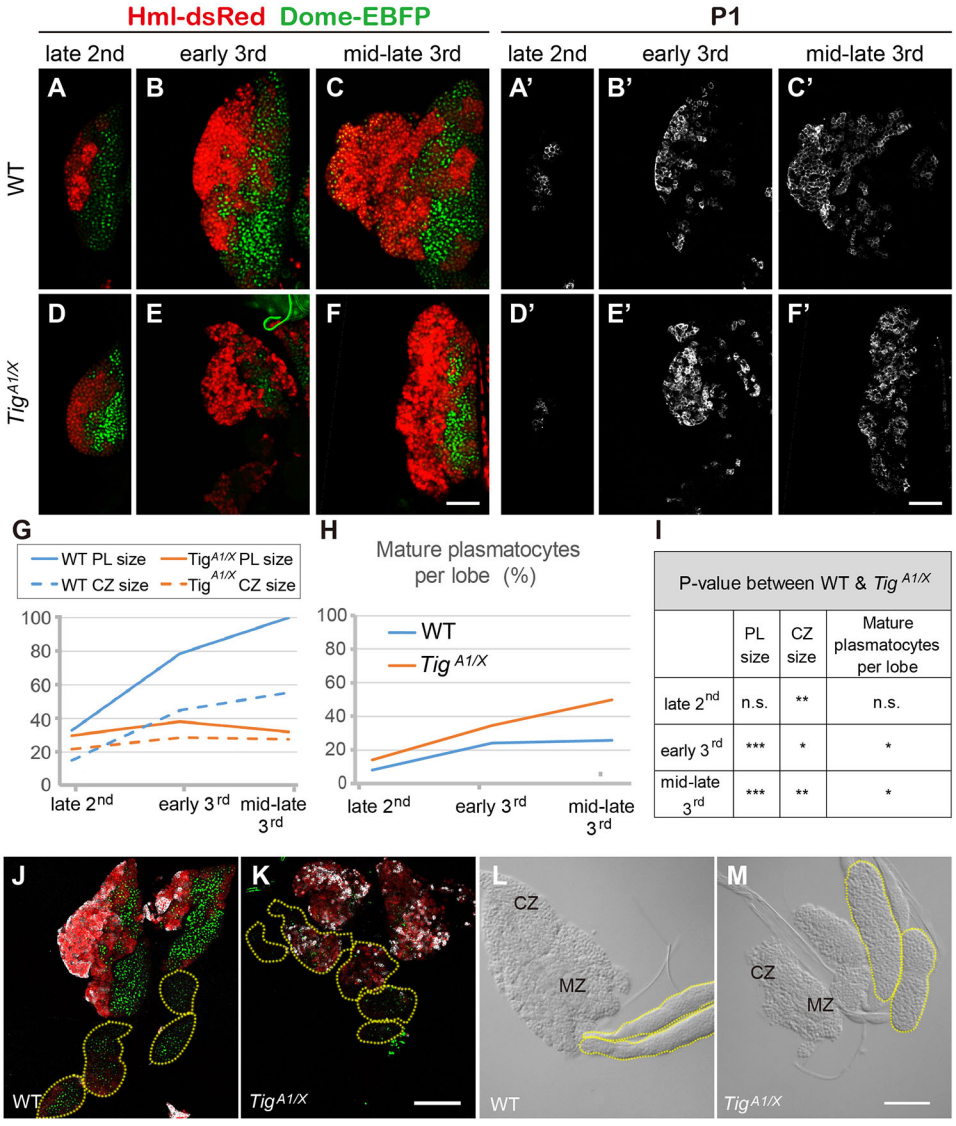

Fig. 2. *Tig* mutants display precocious differentiation of plasmatocytes in the 1° and 2° lobes of the LG. (A-F′) Confocal images of PLs from late 2nd (A,D), early 3rd (B,E) and mid/late 3rd (C,F) instar larvae from *w*^{1118} (A-C) or *Tig*$^{A1/X}$ mutants (D-F). The CZ and MZ are marked by Hml-dsRed (red) and Dome-EBFP (green), respectively (A-F), and plasmatocytes via P1 immunostaining (A′-F′). (G) The decrease in PL and CZ size in the *Tig* mutants manifested during the 3rd instar larval stage. (H) The precocious appearance of P1^{+} plasmatocytes in *Tig* mutants began in early 3rd instars. Data are mean values. (I) Summary of the statistical analysis in G,H. *P<0.05, **P<0.01, ***P<0.001, n.s., not significant. More information on these data is available in Table S2. (J,K) Confocal images of mid 3rd instar larval LGs of wild type and *Tig* mutants in which the 2° lobes are highlighted (yellow dashed lines), marked by Hml-dsRed (red), Dome-EBFP (green) and immunostained for P1 protein (white). The 2° lobes of *Tig* mutants have higher P1 staining and Hml-dsRed expression. (L,M) DIC images of control and *Tig* mutant 2° lobes (yellow dashed lines). Most 2° lobes of wild-type animals displayed smooth tightly packed cells, similar to the MZ of the PL. In contrast, cells in the 2° lobes of most *Tig* mutants appeared larger and more loosely packed, as is typically found in the CZ of the PL. Further description of the phenotypic range of the 2° lobes is provided in Table S3. Scale bars: 50 µm.

Development (2017) 144, 2415-2427 doi:10.1242/dev.149641

To determine whether the precocious maturation of plasmatocytes was specific for loss of *Tig*, rescue via Hml>Tig was performed. Indeed, the phenotype was rescued by heterologous expression of Tig (Fig. 3I-L). *Tig* mutants had higher levels of mature plasmatocytes than wild-type or rescued PLs whether quantified by % $P1^+$ cells/CZ (Fig. 3K) or % $P1^+$ cells/PL (Fig. 3L). In contrast to control and *Tig* rescued PLs, where $P1^+$ cells were also Hml^+, in *Tig* mutants there were $P1^+$ cells that were Hml^- (arrows in Fig. 3E). These $P1^+Hml^-$ cells may represent 'hyper-mature' plasmatocytes that have passed through the $P1^+Hml^+$ stage.

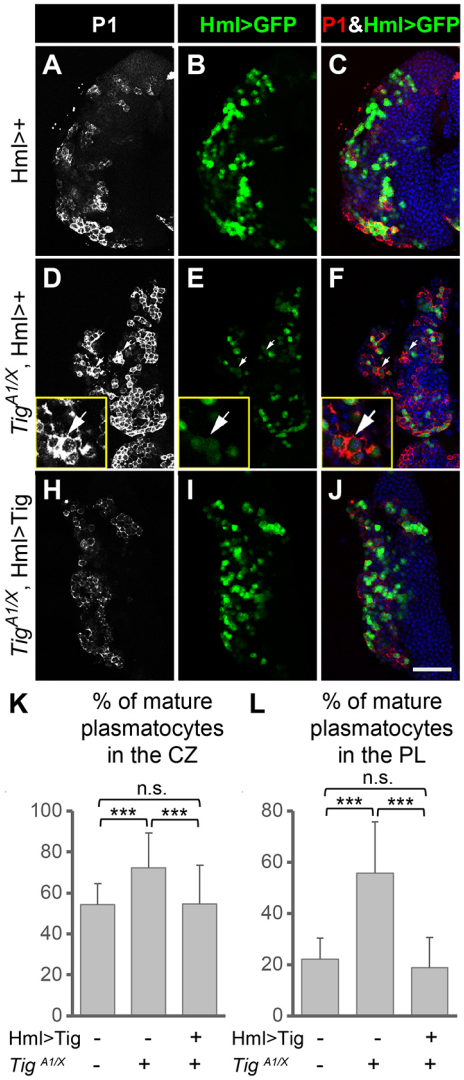

Fig. 3. Rescue of the precocious plasmatocyte differentiation in *Tig* mutants by Hml>Tig. (A-J) Confocal images of PLs from mid 3rd instar larvae containing P[Hml-Gal4] and P[UAS-GFP] in a control (A-C) or a $Tig^{A1/X}$ background without (D-F) or with (H-J) P[UAS-Tig]. Plasmatocytes were marked by P1 staining (white in A,D,H; red in C,F,J), DAPI (blue) and GFP (green). Loss of *Tig* resulted in an increase in $P1^+$ mature plasmatocytes (D) that was rescued in a Hml>Tig background (H). $P1^+$, Hml>GFP^- cells are present in the Tig mutants (arrows in D-F; see also insets). (K) Quantification of the data, using the ratio of $P1^+$, Hml>GFP^+/Hml>GFP^+ cells to determine the percentage of mature plasmatocytes/CZ. (L) Quantification of the data, normalizing the $P1^+$ area to the entire PL, which includes the $P1^+$, Hml>GFP^- cells. Animals were reared at 25°C to restrict Hml>Tig expression to a moderate level. n.s., not significant; ***P<0.001. Nine PLs were examined for each condition. Data are mean±s.e.m. Scale bar: 50 µm.

The *Tig* plasmatocyte phenotype does not appear to be related to increased apoptosis, as expression of the caspase inhibitor P35 did not decrease the frequency of $P1^+$ cells nor rescue PL size defect of *Tig* mutants (Fig. S4). Tig specifically affected plasmatocytes, as no significant difference in the number of lamellocytes or crystal cells were detected in Tig^X/Tig^{A1} PLs (Fig. S5). However, partial knockdown of Tig with RNAi did not recapitulate the plasmatocyte phenotype (Fig. S6) and mutant clones of Tig^X did not display a detectable cell autonomous increase in $P1^+$ cells (Fig. 4). The negative data with RNAi could be due to residual Tig in the PL, whereas the lack of increased plasmatocytes within the mutant clones could be due to non-autonomous rescue from Tig secreted from surrounding cells. Alternatively, these results could mean that loss of Tig in non-PL cells, e.g. circulating or sessile hemocytes are responsible for the PL phenotype (see Discussion for further comment).

Tig overexpression inhibits plasmatocyte maturation

Hml>Tig animals reared at 25°C had no obvious differences in plasmatocyte differentiation (Fig. S7), but increasing the level of Tig expression (via culturing at 29°C) caused a dramatic reduction in the number of $P1^+$ cells (Fig. 5A,F), while having no effect on the CZ marker Hml>GFP (Fig. 5B,G). The level of Tig expression in Hml>Tig PLs was much higher than controls (Fig. 5C,H; Fig. S8), but the residual $P1^+$ cells had no detectable Tig signal (Fig. 5J). Quantification of either optical slices or *z*-stacks demonstrated that the reduction of plasmatocytes was significant (Table 1, Table S4). Hml>Tig animals displayed no developmental delay (Fig. S3), were viable as adults and expression of the caspase inhibitor P35 had

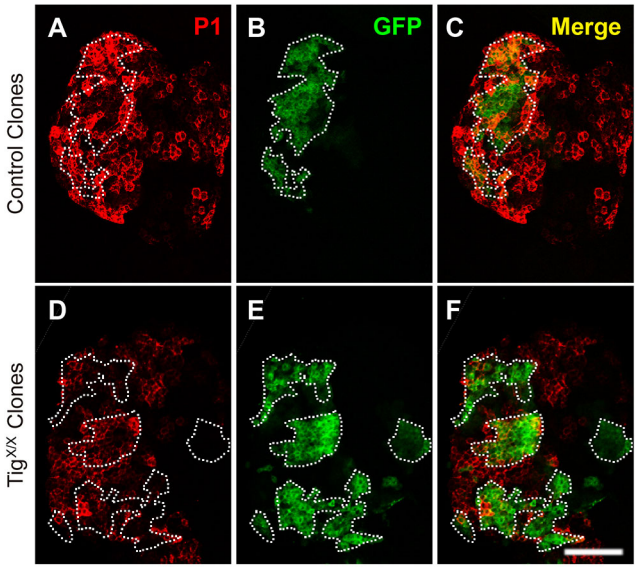

G

% of P1+ cells	# of control clones	# of mutant clones
none	5	6
low	3	4
medium	14	14
high	1	0

Fig. 4. *Tig* mutant clones in the PL do not display a higher number of plasmatocytes. (A-F) Confocal images of PLs stained for P1 (red) and containing MARCM clones of control (A-C) and Tig^X mutant clones (D-F). Clones are marked by GFP (green). (G) Table summarizing P1 staining levels in control and *Tig* mutant clones. No obvious difference in P1 expression was observed inside the *Tig* mutant clones. Animals were reared at 25°C. Scale bar: 50 µm.

Development (2017) 144, 2415-2427 doi:10.1242/dev.149641

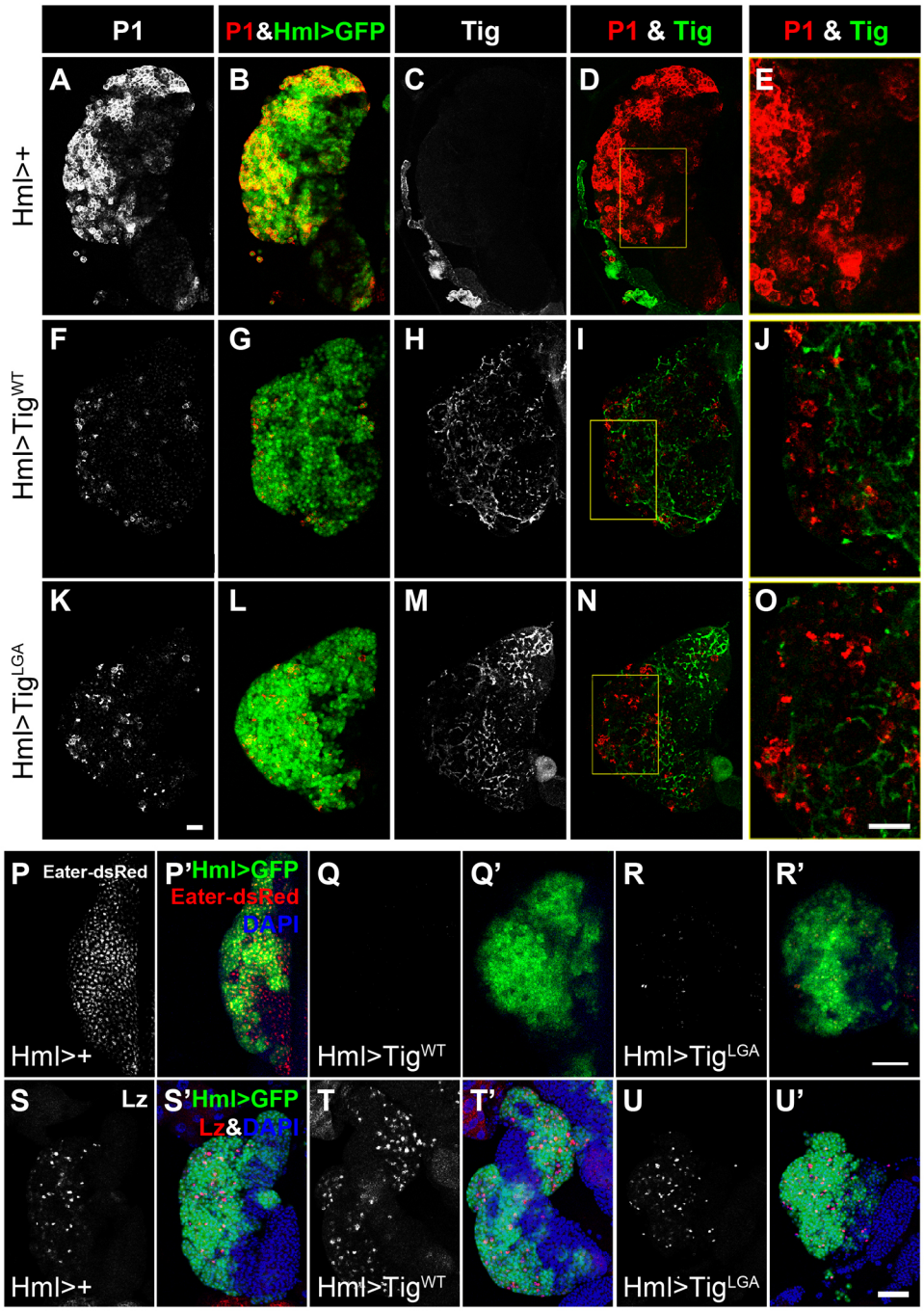

Fig. 5. Tig overexpression represses plasmatocyte differentiation independently of an integrin-binding domain. All confocal images are of PLs from mid/late 3rd instar larvae containing P[Hml-Gal4] and P[UAS-GFP], without or with transgenes expressing wild-type Tig (P[UAS-Tig^{WT}]) or a Tig transgene with a mutated integrin-binding motif (P[UAS-Tig^{LGA}]). (A-O) PLs stained for Tig and P1. When overexpressed at similar levels (C,H,M), both Tig^{WT} and Tig^{LGA} strongly repressed P1 expression (A,F,K). (J,O) Magnification of boxed areas in I and N showing minimal overlap between residual P1 signal and Tig. Quantification of the data is shown in Table 1 and Table S4. (P-R′) PLs containing an Eater-dsRed transgene expressing Tig proteins. Eater-dsRed was strongly repressed by either Tig^{WT} or Tig^{LGA}. (S-U′) PLs stained for the crystal cell marker Lz. Tig^{WT} and Tig^{LGA} did not cause a detectable change in the number of crystal cells (see Fig. S7 for quantification). Animals were reared at 29°C. Scale bars: 25 µm in K for A-D, F-I and K-N; 25 µm in O for E,J,O; 50 µm in R′,U′.

no effect on the ability of Tig to inhibit plasmatocyte maturation (Fig. S9). To confirm the results obtained with P1 immunostaining, we examined a second marker: Eater-dsRed. This reporter is driven by an enhancer from the *Eater* locus, which encodes a phagocytosis receptor expressed specifically in plasmatoctyes (Kocks et al., 2005; Tokusumi et al., 2009). Hml>Tig PLs displayed a strong repression of Eater-dsRed expression (Fig. 5P-Q′). Taken together, these results suggest that overexpression of Tig blocks plasmatocyte differentiation.

During the course of this study, we became aware that several of our stocks contained a mutant allele of *nimC1* (Honti et al., 2013). Importantly, this deletion allele expresses a truncated protein that is not recognized by the P1 antibody. All stocks used in this report contain the wild-type *nimC1* allele, except for the P[Hml-Gal4] P[UAS-GFP] chromosome, the transgenic inserts of which were too close to *nimC1* to recombine away. To examine whether the presence of a mutant *nimC1* allele affected plasmatocyte number, we examined Eater-dsRed expression in the *nimC1* mutants. Interestingly, we found that the *nimC1* mutants had increased Eater-dsRed expression (Fig. S10). In addition, another CZ driver, Pxn-Gal4 (which was wild-type for *nimC1*), also inhibited P1^{+} positive cells when combined with UAS-Tig (Fig. S11). We conclude that the presence of the *nimC1* mutant allele in the Hml-Gal4 experiments does not alter the conclusion that Tig overexpression blocks plasmatocyte maturation.

Based on results from a combination of genetic and biochemical experiments, Tig is a ligand for αPSβPS2 integrin (Brabant et al., 1996; Bunch et al., 1998; Stevens and Jacobs, 2002). Tig contains a

Development (2017) 144, 2415-2427 doi:10.1242/dev.149641

Table 1. Quantification of plasmatocytes in PLs expressing Tig^{WT} or Tig^{LGA}

Genotype	*n*	Plasmatocytes/PL (mean %±s.d.)	*P* value
Hml>+	26	30±15	
Hml>Tig^{WT}	11	17±12	0.0097
Hml>Tig^{LGA}	19	19±13	0.0062

Both wild-type and mutant Tig significantly inhibited $P1^+$ cells.

RGD motif commonly found in integrin ligands (Fogerty et al., 1994). Substitution of these residues (to LGA) greatly reduced integrin-mediated cell spreading and dramatically lowered the ability of transgenic Tig to rescue the muscle attachment defects and lethality of *Tig* mutants (Bunch et al., 1998). However, Tig^{LGA} expression via Hml-Gal4 resulted in the same phenotype, i.e. inhibition of $P1^+$ cells while retaining Hml^+ cells, as Tig^{WT} (Fig. 5K-O; Table 1). Tig^{LGA} and Tig^{WT} also inhibited Eater-dsRed expression similarly (Fig. 5P-R′). Expression levels of both transgenes were similar, as judged by Tig immunostaining (Fig. 5H,M). In addition, overexpression of either Tig had no effect on the frequency of crystal cell formation (Fig. 5S-U′; Fig. S12) or lamellocytes (Fig. S5). These data suggest that Tig specifically inhibits plasmatocyte differentiation in an integrin-independent manner.

Tig prolongs a pre-plasmatocyte, IP cell fate in the PL

Overexpression of Tig in the CZ caused the accumulation of Hml^+ cells that lack the plasmatocyte markers P1 and Eater-dsRed (Fig. 5). They are reminiscent of the IPs that have been previously noted in wild-type PLs (Dragojlovic-Munther and Martinez-Agosto, 2012; Krzemien et al., 2010; Makhijani et al., 2011). Indeed, our examination of Hml>GFP PLs revealed a significant population of cells that were Hml^+ but were $P1^-$ (Fig. 6A-C′). Hml^+ cells with very low levels of P1 staining are also evident (arrow in Fig. 6B). The Hml>GFP signal does not overlap with Lz staining, indicating that the Hml^+ cells were not crystal cells (Fig. 6D-E′). Another line of evidence for the presence of IPs is the existence of cells at the MZ/CZ border that are positive for both MZ and CZ markers (Sinenko et al., 2009; Dragojlovic-Munther and Martinez-Agosto, 2012). Cells with these characteristics (i.e. $Dome^+$, Hml^+) were relatively rare in control PLs, but Hml^+ cells with intermediate levels of Dome signal were readily apparent in the CZ of Hml>Tig PLs (Fig. 6F-I; Table 2). The data indicate that Tig expression causes a buildup of IPs that cannot proceed with plasmatocyte differentiation.

Tig protein is found throughout the CZ (Zhang et al., 2014), which is seemingly in conflict with a model where Tig promotes an IP fate while inhibiting plasmatocyte maturation. To examine the expression of Tig in more detail, *in situ* hybridization was performed to determine the pattern of *Tig* mRNAs. This analysis revealed the presence of significant levels of *Tig* transcripts in both the MZ and CZ, although expression is higher in the CZ (Fig. S13). Examination of the *Tig* transcriptional reporters minR-*lacZ* and Tig-*lacZ* also revealed a complex expression pattern (Fig. 7). Tig-*lacZ*, containing a 1.8 kb stretch of genomic DNA that included sequences upstream of the *Tig* endogenous promoter and the first intron (Zhang et al., 2014), was expressed in the IP and adjacent MZ cells, but was most prominently found in the CZ (Fig. 7A-C,M; Table S5). minR-*lacZ*, containing two repeats of a 40 bp minimal Wg-responsive element from the *Tig* first intron (Zhang et al., 2014), had a more patchy expression where ∼40% of the pattern overlapped with the MZ and IP (Fig. 7G-I,M; Table S5). The Tig-*lacZ* reporter displayed greater overlap with P1 than did minR (Fig. 7D-F,J-L,M,O). Strikingly, although nearly 60% of minR-*lacZ* expression was found in the CZ (Table S5) fewer than 20% of $P1^+$ cells expressed this reporter (Fig. 7O). These data indicate that although the Tig expression pattern overlaps with mature plasmatocytes, *Tig* transcription also occurs in the MZ and IPs.

To examine the effect of Tig overexpression in the MZ, Dome-Gal4 was crossed to a strong UAS-Tig line. Dome>Tig PLs

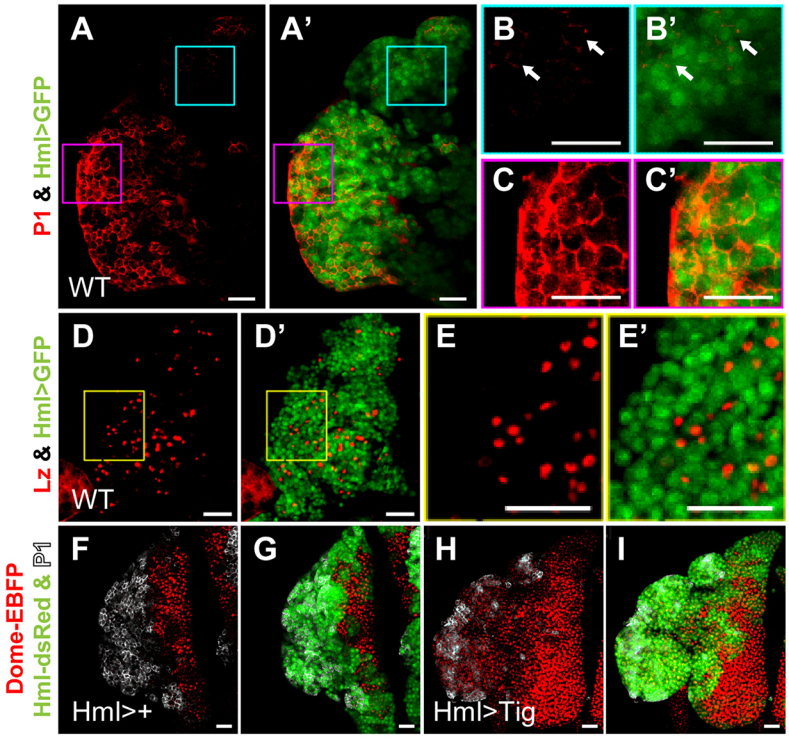

Fig. 6. PLs contain a pool of $Hml^+/P1^-$ IPs that is expanded by Tig expression. Confocal images of PLs from mid/late 3rd instar larvae. (A,A′) Stack projections of the surface layer of a P[Hml-Gal4]/P[UAS-GFP] PL with GFP (green) and P1 immunostaining (red). (B-C′) Magnified views illustrating areas with mostly IPs, i.e. GFP^+ with no detectable P1 (B,B′; arrows indicate cells with low P1 levels) or largely mature plasmatocytes, i.e. GFP^+ $P1^+$ (C,C′). (D-E′) Stack projection of the surface layer of a wild-type PL expressing Hml>GFP (green) and immunostained for Lz (red). Crystal cells (Lz^+) typically have little or no GFP, suggesting that the IPs are not crystal cells. Twelve PLs were examined for each condition. (F-I) PLs expressing P[Hml-Gal4] with or without P[UAS-Tig], also containing zone markers Hml-dsRed (green) and Dome-EBFP (red), and stained for P1 (white). Hml>Tig expanded the population of Hml^+ $P1^-$ cells, which also contained intermediate levels of Dome-EBFP. See Table 2 for further quantification. There was also a reproducible increase in Dome-EBFP expression in the MZ (compare F with H), the reason for which is not clear. All animals were reared at 29°C. Scale bars: 25 µm.

Development (2017) 144, 2415-2427 doi:10.1242/dev.149641

Table 2. Quantification of plasmatocytes/CZ and IPs/CZ in PLs expressing Tig or Wee1

Genotype	*n*	Plasmatocytes/CZ (mean %±s.d.)	*P* value	IP cells/CZ (mean %±s.d.)	*P* value
Hml>+	15	35±13		23±9	
Hml>Tig	17	13±9	3.56×10^{-6}	89±14	1.37×10^{-12}
Hml>+	10	29±12		23±9	
Hml>Wee1	12	17±8	0.038	65±16	6.01×10^{-8}

The percentages of plasmatocytes/CZ were defined by P1$^+$ Hml$^+$/Hml$^+$. The percentages of IPs/CZ were defined by Dome$^+$ Hml$^+$/Hml$^+$. Expression of either Tig or Wee1 significantly decreased plasmatocyte number and increased the number of IPs.

displayed a similar reduction in plasmatocytes as Hml>Tig (Fig. S14). However, Tig immunostaining revealed that Tig protein was detectable only in the CZ (Fig. S14). These results suggest zone-specific regulation of Tig protein, i.e. CZ-specific translation of *Tig* mRNA or MZ-specific degradation of Tig protein. Although the mechanism for these observations requires further investigation, overall these data combined with the *Tig* transcript and transcriptional reporter analysis suggest multiple levels of regulation of Tig expression in the PL, which is not inconsistent with a role in acting as a brake on plasmatocyte maturation.

G_2/M regulators control plasmatocyte differentiation and Tig expression

Hml>Tig PLs had a higher S-phase index than controls (Fig. S15), suggesting that Tig is promoting cell proliferation. However, Hml>Tig PLs also had a dramatic reduction in M-phase index (Fig. S16), suggesting many cells are arrested in G_2 phase. Given that Tig affects both plasmatocyte maturation and cell cycle progression in the PL, we wondered whether these two processes were related, e.g. whether manipulation of cell cycle regulators affected PL cell fate. By screening a collection of known cell cycle regulators, we discovered that expression of Wee1 kinase had a profound effect on plasmatocyte differentiation (Fig. 8). Wee1 regulates G_2/M transition by inhibiting Cdk1, the kinase subunit of maturation-promoting factor (MPF), which promotes the onset of M phase (Campbell et al., 1995; Price et al., 2002; Russell and Nurse, 1987). Hml>Wee1 PLs had a reduction in the number of plasmatocytes (Fig. 8A-H; Table 2 and Table S4), with no significant change in crystal cells and lamellocytes (Fig. 8I-L; Figs S5 and S12). As observed with Tig overexpression, Wee1 caused an accumulation of IPs in the PL (Table 2).

To confirm that Wee1 expression caused a slowdown of the G_2/M transition, we used the RGB cell cycle tracker (Handke et al., 2014). Wee1 caused a marked increase in cells that were positive for EBFP, Tomato and EGFP (arrowheads in Fig. S17), indicative of late G_2 (Handke et al., 2014). Interestingly, the slowing of the G_2/M transition did not reduce the number of Hml$^+$ cells, perhaps owing to increased proliferation of MZ cells (Fig. S17).

To extend the Wee1 results, we examined PLs expressing String/CDC25 (Stg), a phosphatase that antagonizes Wee1 function to activate Cdk1 (Edgar and O'Farrell, 1990; Russell and Nurse, 1986). Hml>Stg phenocopied *Tig* mutants, i.e. PLs were smaller than controls with an increase in mature plasmatocytes (Fig. 9A-F). Interestingly, Hml>Stg PLs had a significant reduction in minR-*lacZ* expression (Fig. 9G-K). Taken together, the Wee1 and Stg data link the G_2/M transition to Tig expression and plasmatocyte differentiation.

The similarity between the Tig and G_2/M phenotypes raised the possibility that they act in a linear pathway. To test this, epistasis

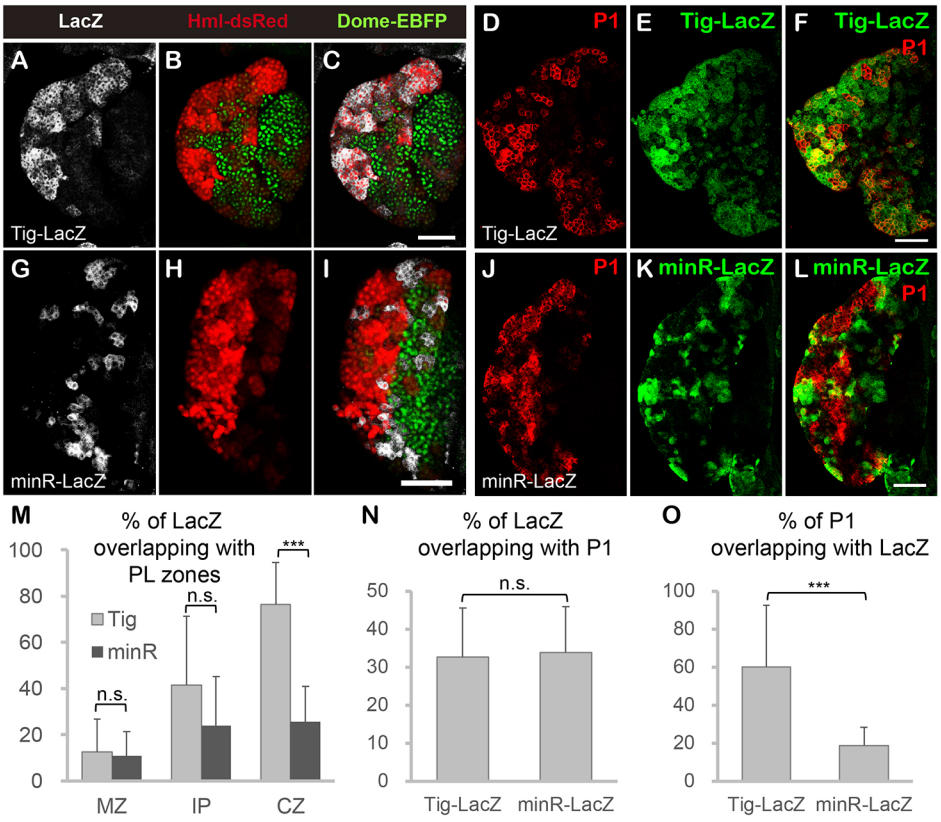

Fig. 7. Expression patterns of *Tig* transcriptional reporters in the PL. (A-L) Confocal images of wild-type PLs expressing Tig-*lacZ* (A-F) or minR-*lacZ* (G-L). PLs were labeled with Hml-dsRed and Dome-EBFP (A-C,G-I, mid/late 3rd instar) or immunostained for P1 (D-F,J-L, mid 3rd instar). Tig-*lacZ* was predominantly found in the CZ (A-C) but many P1$^+$ cells did not express Tig-*lacZ* (D-F). minR-*lacZ* had a patchier expression pattern and was clearly found in both MZ and CZ (G-I), and most of the P1$^+$ cells were not minR-*lacZ*$^+$ (J-L). (M) Quantification of the data showing that both reporters were more likely found in IPs and the CZ rather than the MZ. More information on the quantification can be found in Table S5. (N,O) Quantification from D-F and J-L showing the degree of overlap between the *lacZ* reporters and P1. n.s., not significant; ***P<0.001. Seven PLs were examined for Tig-*lacZ* and 22 for minR-*lacZ*. Data are mean±s.e.m. Scale bars: 50 µm.

Development (2017) 144, 2415-2427 doi:10.1242/dev.149641

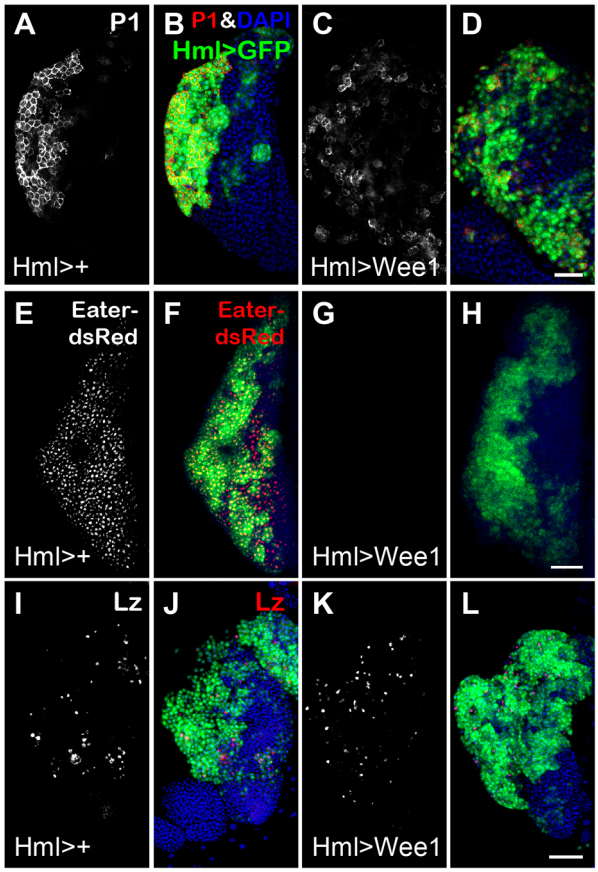

Fig. 8. Wee1 kinase blocks plasmatocyte differentiation. (A-L) Confocal images of PLs from mid/late 3rd instar larvae containing P[Hml-Gal4] and P[UAS-GFP] with or without P[UAS-Wee1] labeled with different cell fate markers. In Hml>Wee1 PLs, P1 (A-D) and Eater-dsRed (E-H) signals were strongly repressed, whereas Lz (I-L) displayed no detectable difference. See Table 2 and Fig. S7 for quantification. Animals were reared at 29°C. Scale bars: 50 µm.

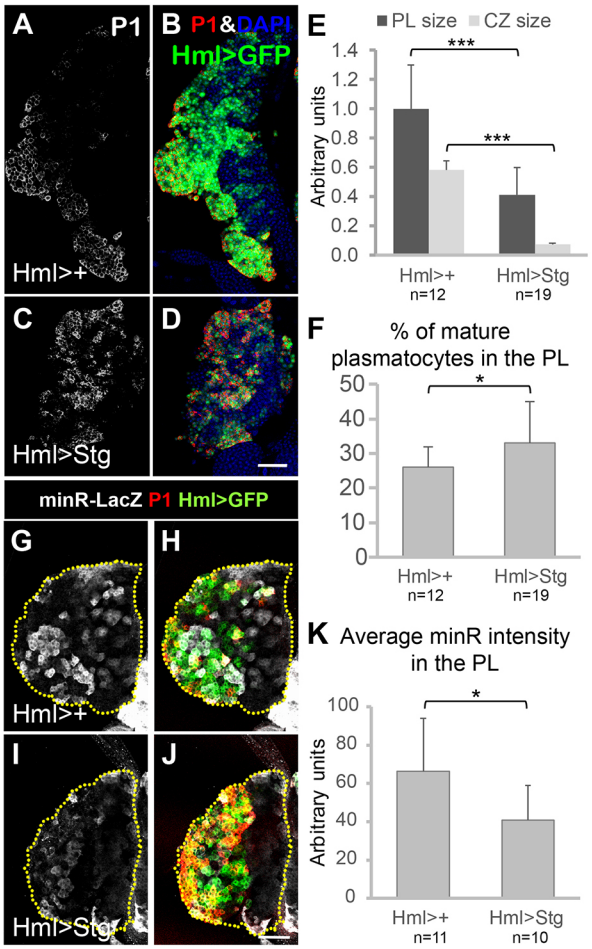

Fig. 9. The phosphatase Stg promotes plasmatocyte differentiation and inhibits Tig reporter expression. (A-D) Confocal images of mid/late 3rd instar PLs containing P[Hml-Gal4] and P[UAS-GFP] with or without P[UAS-Stg], and immunostained for P1. In Hml>Stg PLs, the vast majority of Hml>GFP^{+} cells were also P1^{+}, and the IP population (GFP^{+}, low/no P1) was greatly reduced. (E) Quantification confirmed that PL and CZ sizes were greatly reduced in Hml>Stg PLs. (F) Quantification of P1 staining demonstrated an increase in mature plasmatocytes in Hml>Stg PLs. (G-J) Confocal images of mid 3rd instar PLs containing the minR-*lacZ* reporter, along with P[Hml-Gal4] and P[UAS-GFP] with or without P[UAS-Stg]. Stg expression inhibited minR-*lacZ* expression. (K) Quantification of the data in G-J. All animals were reared at 29°C. Data are mean±s.e.m. **P*<0.05; ****P*<0.001. Scale bars: 50 µm.

analysis was performed by overexpressing Wee1 in a *Tig* mutant background. As described earlier, Hml>Wee1 PLs had a reduced number of mature plasmatocytes (Fig. 10A-D). Conversely, Tig^{A1}/Tig^{X} mutants had a high level of P1^{+} plasmatoctyes (Fig. 10E-H). The composite ($Tig^{A1/X}$, Hml>Wee1) phenotype was very similar to the *Tig* mutant alone, i.e. numerous mature plasmatocytes and very few IPs (Hml^{+}, no/low P1) (Fig. 10I-L; Table 3). These data suggest that Tig acts downstream of Wee1 in regulating the plasmatocyte cell fate.

One possibility to explain our epistasis data is that Wee1 activates Tig expression. Indeed, Tig protein and the Tig transcriptional reporters were dramatically upregulated in a Hml>Wee1 background (Fig. 10M-T), demonstrating that Wee1 expression transcriptionally activated Tig expression. Taken together, the data strongly support a model where the G_2/M transition regulator Wee1 represses plasmatocyte differentiation through inducing Tig expression.

DISCUSSION

In this report, we demonstrated that the ECM protein Tig is an important negative regulator of plasmatocyte maturation in the LG of *Drosophila* (Fig. 11A). Overexpression of Tig inhibited the differentiation of plasmatocytes and *Tig* mutant primary and secondary lobes had precocious maturation of these macrophage-like cells. These manipulations in *Tig* gene activity had little or no effect on non-plasmatocyte lineages, i.e. crystal cell and lamellocytes. *Tig* mutant phenotypes were rescued by expression of transgenic Hml>Tig. Hml-Gal4 is active in the CZ of the PL, but also in circulating and residual hemocytes outside the LG (Goto et al., 2003; Makhijani et al., 2011). Given that Tig is expressed in the CZ of the PL (Zhang et al., 2014; Fig. 10M, Figs S6, S8 and S14), the simplest explanation is that Tig expressed in the LG is responsible for regulating plasmatocytes. But our data do not exclude the possibility that Tig expressed in non-LG cells could also contribute to the phenotypes we observed. In any case, our work demonstrates that, in addition to its function in muscle attachment (Bunch et al., 1998), Tig plays an important role in regulating cell fate specification during hematopoiesis in the LG.

Prohemocytes in the MZ (e.g. marked by Dome-EBFP) transition to hemocytes through IPs that contain residual Dome-EBFP and CZ markers such as Hml>GFP (Dragojlovic-Munther and Martinez-

Development (2017) 144, 2415-2427 doi:10.1242/dev.149641

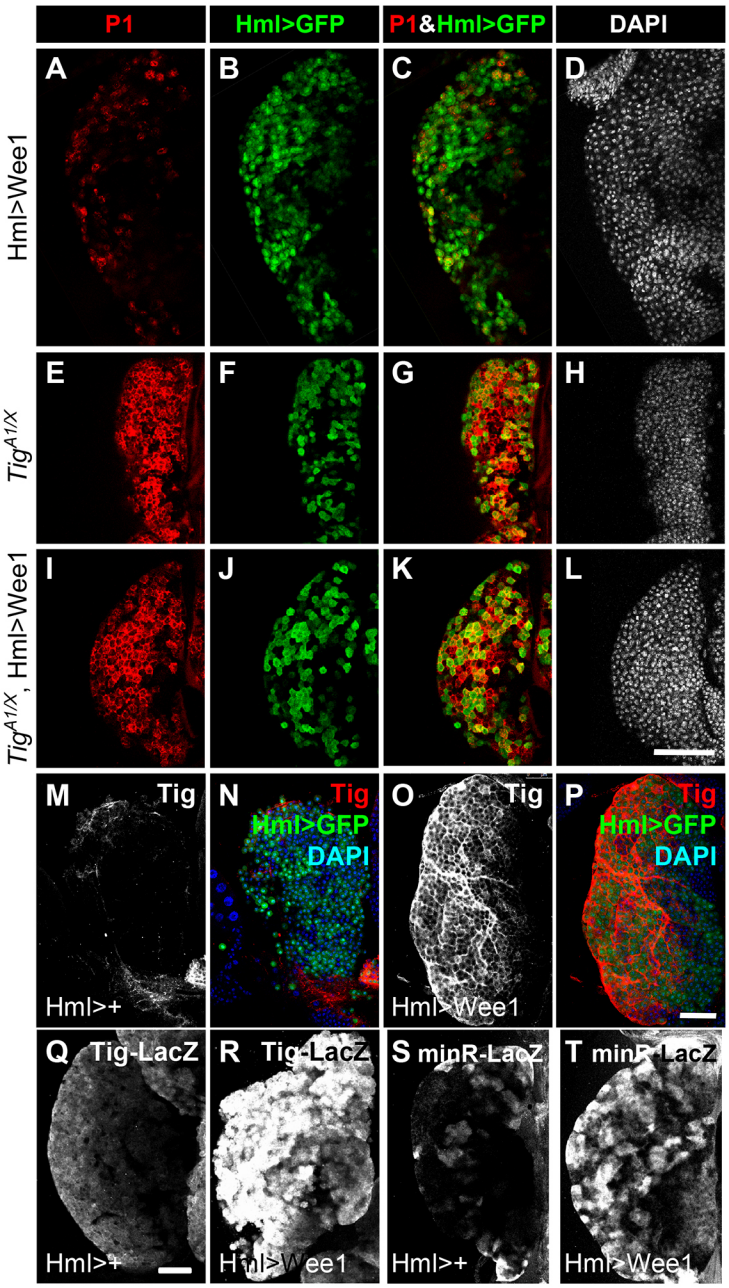

Fig. 10. Wee1 regulates plasmatocyte differentiation through Tig expression. Confocal images of PLs from mid/late 3rd instar larva. All PLs contained P[Hml-Gal4] and P[UAS-GFP] with or without P[UAS-Wee] and *Tig* mutant alleles. (A-D) The CZ (Hml>GFP$^+$) of Hml>Wee1 PLs had few plasmatocytes (GFP$^+$ P1$^+$) and many IPs (GFP$^+$ low/no P1). (E-L) The CZ of *Tig* mutant PLs, with or without Wee1 overexpression, had high levels of mature plasmatocytes and few IPs. See Table 3 for quantification. (M-T) PLs containing P[Hml-Gal4] and P[UAS-GFP] with or without P[UAS-Wee1]. Wee1 induced strong activation of Tig protein (compare M with O) in 50% of PLs examined (n=12). For Tig-*lacZ*, strong Wee1-dependent activation of the reporter (compare Q with R) was observed in 75% of PLs (n=12). For minR-*lacZ*, strong induction (compare S with T) was observed in all PLs (n=10). All animals were reared at 29°C. Scale bars: 50 µm.

Agosto, 2012; Sinenko et al., 2009). Cells closer to the periphery of the CZ tend to express increasing levels of P1, a plasmatocyte marker (Krzemien et al., 2010; Makhijani et al., 2011) (Fig. 6A-C′). Thus, the prohemocytes in the MZ are Dome$^+$, Hml$^-$ and P1$^-$, IPs are Dome$^+$, Hml$^+$ and P1$^-$, and maturing plasmatocytes are Dome$^-$, Hml$^+$ and P1$^+$ (Fig. 11B). Overexpression of Tig in the CZ 'freezes' many cells in the IP fate, leading to an accumulation of cells expressing high levels of Hml reporters and intermediate levels of Dome-EBFP (Fig. 11B).

Our results suggest that Tig slows down plasmatocyte differentiation in the CZ, which could allow the formation of sufficient progenitors to generate the appropriate number of plasmatocytes. This model predicts that Tig expression would be highest in IPs, but this is not supported by immunostaining data (Zhang et al., 2014) and the analysis of *Tig* transcripts and transcriptional reporters in this report. One possibility is the existence of a 'regulatory' pool of Tig that is predominately active in IPs (Fig. 11C). Perhaps this regulatory pool comprises newly synthesized Tig, which can influence plasmatocyte maturation before it becomes incorporated into the ECM. An alternative explanation is that Tig is permissive for blocking plasmatocyte differentiation, and other unidentified factor(s) exist that inhibit plasmatocyte maturation and are localized to the IP compartment.

How does Tig inhibit plasmatocyte differentiation?

Tig contains an Arg-Gly-Glu (RGD) motif towards its C terminus, which was required for integrin binding in a cell-spreading assay (Bunch et al., 1998). Mutation of this tripeptide motif (RGD to LGA) greatly reduced the ability of a transgene to rescue the muscle attachment phenotype of *Tig* mutants (Bunch et al., 1998). However, we found that the Tig^{LGA} transgene had no detectable defect in

Development (2017) 144, 2415-2427 doi:10.1242/dev.149641

Table 3. Quantification of the Hml>Wee1, Tig$^{A1/X}$ epistasis data

Genotype	*n*	Plasmatocytes/CZ (mean %±s.d.)	*P* value (versus Hml>Wee1)	*P* value (versus TigA1/X)
Hml>Wee1	6	17±7.9	NA	0.009
Tig$^{A1/X}$	13	94±41	0.009	NA
Hml>Wee1; *Tig*$^{A1/X}$	12	75±21	4.70×10^{-6}	0.083

The percentage of plasmatocytes/CZ was defined by P1^{+} Hml^{+}/Hml^{+}. Compound PLs lacking *Tig* and overexpressing Wee1 were similar to *Tig* mutants and distinct from Hml>Wee1.

blocking plasmatocyte differentiation. Although we cannot exclude the possibility that the LGA mutation retains the ability to bind to some integrin heterodimers, these data suggest that Tig regulates plasmatocyte differentiation independently of integrin signaling.

Are there other factors that regulate plasmatocyte development in *Drosophila* that could work in concert with Tig? While screening for suppressors of a LG overgrowth phenotype, three genes, *visgun* (*vsg*), *SHC-adaptor protein* (*shc*) and *Adenosine deaminase-related growth factor A* (*Adgf-A*), were identified where loss of function results in precocious plasmatocyte differentiation (Tan et al., 2012). *vsg* encodes an ortholog of mammalian endolyn, a endolysosomal sialomucin (Zhou et al., 2006) and *shc* encodes a SH2/PTB adaptor protein required for a subset of receptor tyrosine kinase receptors (Luschnig et al., 2000). Adgf-A expression is activated by JAK/STAT signaling in the CZ, which lowers extracellular adenosine levels in the MZ, maintaining the prohemocyte population (Mondal et al., 2011, 2014). The GATA transcription factor *pannier* (*pnr*) promotes plasmatocyte differentiation (Minakhina et al., 2011) so it would be possible to examine whether *pnr* is epistatic to *Tig*. Further examination is necessary to determine whether any of these factors act in conjunction with Tig to control plasmatocyte maturation.

Cell cycle regulation and cell fate determination – a case in fly hematopoiesis

Precise coordination between cell cycle progression and cell fate determination is necessary for proper development and tissue homeostasis, e.g. during neural cell lineages (Farkas and Huttner, 2008; Fichelson et al., 2005) and hematopoiesis (Nakamura-Ishizu et al., 2014). In many cases, cells exit the cell cycle upon terminal differentiation (Buttitta and Edgar, 2007) and perturbations that prolong cell cycle progression result in premature differentiation (Manansala et al., 2013; Tapias et al., 2014). Here, we report a particularly dramatic example where the specification of the plasmatocyte cell fate is tightly controlled by regulators of the G_2/M transition, namely Wee1 and Stg. Interestingly, forced expression of Cdc25a (a vertebrate homolog of Stg) in zebrafish embryos blocks muscle differentiation (Bouldin et al., 2014). This is the opposite of what we observe, i.e. Stg overexpression promotes premature formation of plasmatocytes (Fig. 9). In pluripotent stem cells, cells in G_1 phase are more likely to undergo differentiation (Bouldin and Kimelman, 2014; Calder et al., 2013; Coronado et al., 2013; Sela et al., 2012), possibly owing to cell cycle stage-dependent expression of key developmental regulators (Pauklin and Vallier, 2013; Singh et al., 2015). Perhaps our data showing that Wee1 and Stg regulate Tig expression is an example of G_2 phase-dependent developmental regulation.

Although it is possible that Wee1 and Stg regulate plasmatocyte differentiation through their ability to regulate the cell cycle, other mechanisms are also possible. There is some evidence that Cyclin-dependent kinase 1 (Cdk1), the target of Wee and Stg (Fig. 11A), affects gene expression through phosphorylation of transcription factors (Lim and Kaldis, 2013; Hu et al., 2009, 2011). The fact that Wee1 and Stg regulate expression of minR-*lacZ*, a synthetic reporter that contains two TCF/Pan-binding sites (from the *Tig* regulatory region) placed upstream of a minimal promoter (Zhang et al., 2014), suggests that Wee1 and Stg influence *Tig* transcription via a mechanism that involves TCF/Pan or a factor that associates with this Wnt-regulated transcription factor. Further studies of this

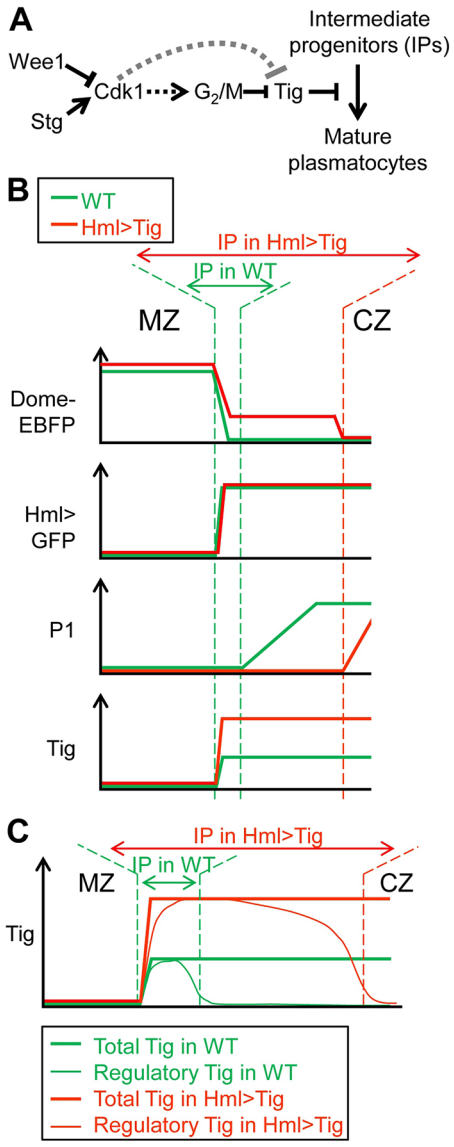

Fig. 11. Working model of the regulation of plasmatocyte maturation by Tig and cell cycle regulators. (A) Genetic pathway controlling plasmatocyte differentiation. Tig and Wee1 inhibit the transition from IPs to plasmatocytes, while Stg accelerates it. Tig is epistatic to Wee1 and Wee1 activates Tig expression. Wee1 and Stg could affect Tig though their common target Cdk1 and may affect Tig expression by altering the G_2/M transition. Alternatively, they could act on *Tig* transcription independently of the cell cycle. (B) Summary of the expression levels of different proteins across the MZ and CZ in wild-type and Hml>Tig PLs at the mid/late-3rd instar stage. There is a dramatic expansion of the domain containing IPs in Hml>Tig, i.e. cells that are Dome^{+}/Hml^{+}/P1^{-}. (C) A speculative model for a 'regulatory' pool of Tig promoting the IP cell fate. Tig protein is detected at uniform levels throughout the CZ (Zhang et al., 2014), but we propose that newly synthesized Tig protein forms a regulatory pool that is enriched in the IPs, where it acts as a brake on plasmatocyte maturation.

Development (2017) 144, 2415-2427 doi:10.1242/dev.149641

regulation will deepen our understanding of hematopoiesis and shed additional light on the connection between the cell cycle and cell fate determination.

MATERIALS AND METHODS

Drosophila stocks

pUAST-Tig^{WT} and pUAST-Tig^{LGA} plasmids were provided by Thomas Bunch (University of Arizona, Tucson, AZ, USA) (Bunch et al., 1998). Transgenic flies were generated by Rainbow Transgenic Flies (Camarillo, CA, USA) in a w^{1118} background. A pair of P[UAS-Tig^{WT}] and P[UAS-Tig^{LGA}] flies with similar relatively strong expression levels were used for all further experiments. For the rescue of *Tig* mutants, cultures containing P[UAS-Tig] transgenes were maintained at 25°C; in all other experiments, cultures were grown at 29°C to achieve significantly higher expression.

The other fly stocks used in this study were: Tig^{X} and Tig^{A1} (Bunch et al., 1998); Hml-Gal4 (Goto et al., 2003); Domeless-Gal4 (Dome-Gal4) (Bourbon et al., 2002); UAS-Wee1 (Price et al., 2002); UAS-Stg (Neufeld and Edgar, 1998); UAS-RGB (Handke et al., 2014); Tig-*lacZ* and minR-*lacZ* (Zhang et al., 2014); Eater-dsRed (Kocks et al., 2005; Tokusumi et al., 2009); DHH, a line containing Dome-EBFP2, Hml-DsRed and hedgehog-GFP reporters (Evans et al., 2014); a Viking/Collagen IV gene trap (Vkg-GFP; Morin et al., 2001); Peroxidase-Gal4 (Pxn-Gal4; Stramer et al., 2005); UAS-P35 (Mergliano and Minden, 2003); and Serpent-Gal4 (Srp-Gal4; Huelsmann et al., 2006). The P[UAS-TigRNAi] is from the Vienna Drosophila Resource Center (#100036).

The Tig^{X} mutant allele was recombined onto a FRT^{40A} chromosome as previously described (Xu and Rubin, 1993). Mutant clones were generated using the MARCM system, using a P[HS-FLP^{122}] P[Tub-Gal4] P[UAS-GFP]; P[Tub-Gal80^{ts}] FRT^{40A} stock kindly provided by Chung-Yu Lee (University of Michigan, Ann Arbor, MI, USA). A FRT^{40A} chromosome was used as a control. Clones were induced by a 1 hour heat shock at 37°C at 48-60 h AEL, and larva were dissected, fixed and analyzed 48 h later.

All crosses were initiated at 25°C. Embryos were collected within a 12 h window, transferred at 24-36 h AEL to 29°C if necessary and dissected at desired time (60-72 h AEL for late 2nd instar, 72-84 h for early 3rd instar, 90-102 h for mid 3rd instar, 96-108 h for mid/late 3rd instar and 102-114 h for late 3rd instar). See supplementary Materials and Methods for further details.

Immunohistochemistry and *in situ* hybridization

For PL/LG dissection, previously described protocols were used for immunostaining (Lebestky et al., 2000) or imaging of fluorescent markers (Small et al., 2012). Immunostaining was carried out as previously described (Zhang et al., 2014). Primary antibodies were used at the following dilutions: mouse α-P1 at 1:75, mouse α-L1 at 1:10 (Kurucz et al., 2007), mouse α-Lz at 1:30 (Lebestky et al., 2000; obtained from Developmental Studies Hybridoma Bank, DSHB), rabbit α-Tig at 1:50 (Deng et al., 2010), mouse α-Cut at 1:100 (Blochlinger et al., 1990; Ab 2B10, deposited by G. Rubin at DSHB) and rabbit α-*lacZ* (MP Biomedicals, 0855976) at 1:1000. Antisense digoxigenin-labeled probe against *Tig* mRNA was synthesized as previously described (Blauwkamp et al., 2008). See supplementary Materials and Methods for further details.

Imaging and data quantification

All fluorescent micrographs were taken with a Leica SP5 laser scanning confocal microscope. Bright-field imaging was conducted with a Nikon Eclipse E600 microscope. All images, except for Fig. 6A-C′, are thin optical slices, with P1 slices taken approximately one-third of the way into the PL from the dorsal side (where the Hml>GFP^{+}, low/no P1 population of cells is the most obvious) and Lz slices taken approximately half way through the PL (where the most Lz^{+} cells are found). The number of PLs examined are indicated for each figure but were typically more than nine PLs/condition and were obtained in multiple experiments. There was no exclusion of samples and representative images are shown.

Images from optimal slices were quantified without blinding using Adobe Photoshop and ImageJ. For crucial data, i.e. the increase in P1^{+} plasmatocytes in *Tig* mutants and the reciprocal decrease in plasmatocytes caused by overexpression of Tig or Wee1, quantification of volumetric stacks was also performed. In all cases, data obtained from volumetric stacks and optical slices were similar (see Tables S1 and S4). The data are presented as means±s.d. Unpaired *t*-tests were used to determine whether means were statistically different. See supplementary Materials and Methods for further details.

Acknowledgements

We thank Utpal Banerjee, Robert Schulz, Laura Buttitta and the Bloomington *Drosophila* Stock Center for fly stocks. We also thank Thomas Bunch for pUAST-Tig^{WT} and pUAST-Tig^{LGA} plasmids, and Istvan Ando, Andrew Simmonds and the Developmental Studies Hybridoma Bank for primary antibodies. Thanks to Mingxue Gu for the TigRNAi data and Vinson Fan for careful reading of the manuscript. Special thanks to Laura Buttitta and members of the Buttitta lab for stimulating discussions about the link between the cell cycle and cell fate specification and for the use of their Leica DM6000 B upright microscope system.

Competing interests

The authors declare no competing or financial interests.

Author contributions

Conceptualization: C.U.Z., K.M.C.; Methodology: C.U.Z., K.M.C.; Validation: C.U.Z., K.M.C.; Formal analysis: C.U.Z., K.M.C.; Investigation: C.U.Z., K.M.C.; Resources: C.U.Z., K.M.C.; Writing - original draft: C.U.Z.; Writing - review & editing: C.U.Z., K.M.C.; Visualization: C.U.Z., K.M.C.; Supervision: K.M.C.; Project administration: K.M.C.; Funding acquisition: K.M.C.

Funding

This work was funded by grants from the National Institutes of Health (GM108468), American Heart Association (12PRE9520018) and the University of Michigan Comprehensive Cancer Center (G012896). Deposited in PMC for release after 12 months.

Supplementary information

Supplementary information available online at
http://dev.biologists.org/lookup/doi/10.1242/dev.149641.supplemental

References

Alfonso, T. B. and Jones, B. W. (2002). gcm2 promotes glial cell differentiation and is required with glial cells missing for macrophage development in Drosophila. *Dev. Biol.* **248**, 369-383.

Ayyaz, A., Li, H. and Jasper, H. (2015). Haemocytes control stem cell activity in the Drosophila intestine. *Nat. Cell Biol.* **17**, 736-748.

Benmimoun, B., Polesello, C., Haenlin, M. and Waltzer, L. (2015). The EBF transcription factor Collier directly promotes Drosophila blood cell progenitor maintenance independently of the niche. *Proc. Natl. Acad. Sci. USA* **112**, 9052-9057.

Blauwkamp, T. A., Chang, M. V. and Cadigan, K. M. (2008). Novel TCF-binding sites specify transcriptional repression by Wnt signalling. *EMBO J.* **27**, 1436-1446.

Blochlinger, K., Bodmer, R., Jan, L. Y. and Jan, Y. N. (1990). Patterns of expression of cut, a protein required for external sensory organ development in wild-type and cut mutant Drosophila embryos. *Genes Dev.* **4**, 1322-1331.

Bouldin, C. M. and Kimelman, D. (2014). Cdc25 and the importance of G2 control: insights from developmental biology. *Cell Cycle* **13**, 2165-2171.

Bouldin, C. M., Snelson, C. D., Farr, G. H., III and Kimelman, D. (2014). Restricted expression of cdc25a in the tailbud is essential for formation of the zebrafish posterior body. *Genes Dev.* **28**, 384-395.

Bourbon, H.-M., Gonzy-Treboul, G., Peronnet, F., Alin, M.-F., Ardourel, C., Benassayag, C., Cribbs, D., Deutsch, J., Ferrer, P., Haenlin, M. et al. (2002). A P-insertion screen identifying novel X-linked essential genes in Drosophila. *Mech. Dev.* **110**, 71-83.

Brabant, M. C., Fristrom, D., Bunch, T. A. and Brower, D. L. (1996). Distinct spatial and temporal functions for PS integrins during Drosophila wing morphogenesis. *Development* **122**, 3307-3317.

Bunch, T. A., Graner, M. W., Fessler, L. I., Fessler, J. H., Schneider, K. D., Kerschen, A., Choy, L. P., Burgess, B. W. and Brower, D. L. (1998). The PS2 integrin ligand tiggrin is required for proper muscle function in Drosophila. *Development* **125**, 1679-1689.

Buttitta, L. A. and Edgar, B. A. (2007). Mechanisms controlling cell cycle exit upon terminal differentiation. *Curr. Opin. Cell Biol.* **19**, 697-704.

Calder, A., Roth-Albin, I., Bhatia, S., Pilquil, C., Lee, J. H., Bhatia, M., Levadoux-Martin, M., McNicol, J., Russell, J., Collins, T. et al. (2013). Lengthened G1 phase indicates differentiation status in human embryonic stem cells. *Stem Cells Dev.* **22**, 279-295.

Development (2017) 144, 2415-2427 doi:10.1242/dev.149641

Campbell, S. D., Sprenger, F., Edgar, B. A. and O'Farrell, P. H. (1995). Drosophila Wee1 kinase rescues fission yeast from mitotic catastrophe and phosphorylates Drosophila Cdc2 in vitro. *Mole. Biol. Cell* **6**, 1333-1347.

Charroux, B. and Royet, J. (2009). Elimination of plasmatocytes by targeted apoptosis reveals their role in multiple aspects of the Drosophila immune response. *Proc. Natl. Acad. Sci. USA* **106**, 9797-9802.

Coronado, D., Godet, M., Bourillot, P.-Y., Tapponnier, Y., Bernat, A., Petit, M., Afanassieff, M., Markossian, S., Malashicheva, A., Iacone, R. et al. (2013). A short G1 phase is an intrinsic determinant of naïve embryonic stem cell pluripotency. *Stem Cell Res.* **10**, 118-131.

Crozatier, M. and Meister, M. (2007). Drosophila haematopoiesis. *Cell. Microbiol.* **9**, 1117-1126.

Crozatier, M. and Vincent, A. (2011). Drosophila: a model for studying genetic and molecular aspects of haematopoiesis and associated leukaemias. *Dis. Model. Mech.* **4**, 439-445.

Crozatier, M., Ubeda, J.-M., Vincent, A. and Meister, M. (2004). Cellular immune response to parasitization in Drosophila requires the EBF orthologue collier. *PLoS Biol.* **2**, e196.

Deng, H., Bell, J. B. and Simmonds, A. J. (2010). Vestigial is required during late-stage muscle differentiation in Drosophila melanogaster embryos. *Mol. Biol. Cell* **21**, 3304-3316.

Dragojlovic-Munther, M. and Martinez-Agosto, J. A. (2012). Multifaceted roles of PTEN and TSC orchestrate growth and differentiation of Drosophila blood progenitors. *Development* **139**, 3752-3763.

Duvic, B., Hoffmann, J. A., Meister, M. and Royet, J. (2002). Notch signaling controls lineage specification during Drosophila larval hematopoiesis. *Curr. Biol.* **12**, 1923-1927.

Edgar, B. A. and O'Farrell, P. H. (1990). The three postblastoderm cell cycles of Drosophila embryogenesis are regulated in G2 by string. *Cell* **62**, 469-480.

Evans, C. J., Olson, J. M., Ngo, K. T., Kim, E., Lee, N. E., Kuoy, E., Patananan, A. N., Sitz, D., Tran, P. T., Do, M.-T. et al. (2009). G-TRACE: rapid Gal4-based cell lineage analysis in Drosophila. *Nat. Methods* **6**, 603-605.

Evans, C. J., Liu, T. and Banerjee, U. (2014). Drosophila hematopoiesis: markers and methods for molecular genetic analysis. *Methods* **68**, 242-251.

Farkas, L. M. and Huttner, W. B. (2008). The cell biology of neural stem and progenitor cells and its significance for their proliferation versus differentiation during mammalian brain development. *Curr. Opin. Cell Biol.* **20**, 707-715.

Ferguson, G. B. and Martinez-Agosto, J. A. (2014). Yorkie and Scalloped signaling regulates Notch-dependent lineage specification during Drosophila hematopoiesis. *Curr. Biol.* **24**, 2665-2672.

Fichelson, P., Audibert, A., Simon, F. and Gho, M. (2005). Cell cycle and cell-fate determination in Drosophila neural cell lineages. *Trends Genet.* **21**, 413-420.

Fogerty, F. J., Fessler, L. I., Bunch, T. A., Yaron, Y., Parker, C. G., Nelson, R. E., Brower, D. L., Gullberg, D. and Fessler, J. H. (1994). Tiggrin, a novel Drosophila extracellular matrix protein that functions as a ligand for Drosophila alpha PS2 beta PS integrins. *Development* **120**, 1747-1758.

Gold, K. S. and Brückner, K. (2015). Macrophages and cellular immunity in Drosophila melanogaster. *Semin. Immunol.* **27**, 357-368.

Goto, A., Kadowaki, T. and Kitagawa, Y. (2003). Drosophila hemolectin gene is expressed in embryonic and larval hemocytes and its knock down causes bleeding defects. *Dev. Biol.* **264**, 582-591.

Graner, M. W., Bunch, T. A., Baumgartner, S., Kerschen, A. and Brower, D. L. (1998). Splice variants of the Drosophila PS2 integrins differentially interact with RGD-containing fragments of the extracellular proteins tiggrin, ten-m, and D-laminin 2. *J. Biol. Chem.* **273**, 18235-18241.

Grigorian, M., Mandal, L. and Hartenstein, V. (2011). Hematopoiesis at the onset of metamorphosis: terminal differentiation and dissociation of the Drosophila lymph gland. *Dev. Genes Evol.* **221**, 121-131.

Handke, B., Szabad, J., Lidsky, P. V., Hafen, E. and Lehner, C. F. (2014). Towards long term cultivation of Drosophila wing imaginal discs in vitro. *PLoS ONE* **9**, e107333.

Holz, A., Bossinger, B., Strasser, T., Janning, W. and Klapper, R. (2003). The two origins of hemocytes in Drosophila. *Development* **130**, 4955-4962.

Honti, V., Cinege, G., Csordás, G., Kurucz, É., Zsámboki, J., Evans, C. J., Banerjee, U. and Andó, I. (2013). Variation of NimC1 expression in Drosophila stocks and transgenic strains. *Fly* **7**, 263-268.

Honti, V., Csordás, G., Kurucz, É., Márkus, R. and Andó, I. (2014). The cell-mediated immunity of Drosophila melanogaster: hemocyte lineages, immune compartments, microanatomy and regulation. *Dev. Comp. Immunol.* **42**, 47-56.

Hu, M. G., Deshpande, A., Enos, M., Mao, D., Hinds, E. A., Hu, G.-F., Chang, R., Guo, Z., Dose, M., Mao, C. et al. (2009). A requirement for cyclin-dependent kinase 6 in thymocyte development and tumorigenesis. *Cancer Res.* **69**, 810-818.

Hu, M. G., Deshpande, A., Schlichting, N., Hinds, E. A., Mao, C., Dose, M., Hu, G.-F., Van Etten, R. A., Gounari, F. and Hinds, P. W. (2011). CDK6 kinase activity is required for thymocyte development. *Blood* **117**, 6120-6131.

Huelsmann, S., Hepper, C., Marchese, D., Knöll, C. and Reuter, R. (2006). The PDZ-GEF dizzy regulates cell shape of migrating macrophages via Rap1 and integrins in the Drosophila embryo. *Development* **133**, 2915-2924.

Jung, S.-H., Evans, C. J., Uemura, C. and Banerjee, U. (2005). The Drosophila lymph gland as a developmental model of hematopoiesis. *Development* **132**, 2521-2533.

Kocks, C., Cho, J. H., Nehme, N., Ulvila, J., Pearson, A. M., Meister, M., Strom, C., Conto, S. L., Hetru, C., Stuart, L. M. et al. (2005). Eater, a transmembrane protein mediating phagocytosis of bacterial pathogens in Drosophila. *Cell* **123**, 335-346.

Krzemien, J., Oyallon, J., Crozatier, M. and Vincent, A. (2010). Hematopoietic progenitors and hemocyte lineages in the Drosophila lymph gland. *Dev. Biol.* **346**, 310-319.

Kurucz, E., Márkus, R., Zsámboki, J., Folkl-Medzihradszky, K., Darula, Z., Vilmos, P., Udvardy, A., Krausz, I., Lukacsovich, T., Gateff, E. et al. (2007). Nimrod, a putative phagocytosis receptor with EGF repeats in Drosophila plasmatocytes. *Curr. Biol.* **17**, 649-654.

Lanot, R., Zachary, D., Holder, F. and Meister, M. (2001). Postembryonic hematopoiesis in Drosophila. *Dev. Biol.* **230**, 243-257.

Lebestky, T., Chang, T., Hartenstein, V. and Banerjee, U. (2000). Specification of Drosophila hematopoietic lineage by conserved transcription factors. *Science* **288**, 146-149.

Letourneau, M., Lapraz, F., Sharma, A., Vanzo, N., Waltzer, L. and Crozatier, M. (2016). Drosophila hematopoiesis under normal conditions and in response to immune stress. *FEBS Lett.* **590**, 4034-4051.

Lim, S. and Kaldis, P. (2013). Cdks, cyclins and CKIs: roles beyond cell cycle regulation. *Development* **140**, 3079-3093.

Luschnig, S., Krauss, J., Bohmann, K., Desjeux, I. and Nüsslein-Volhard, C. (2000). The Drosophila SHC adaptor protein is required for signaling by a subset of receptor tyrosine kinases. *Mol. Cell* **5**, 231-241.

Makhijani, K., Alexander, B., Tanaka, T., Rulifson, E. and Bruckner, K. (2011). The peripheral nervous system supports blood cell homing and survival in the Drosophila larva. *Development* **138**, 5379-5391.

Manansala, M. C., Min, S. and Cleary, M. D. (2013). The Drosophila SERTAD protein Taranis determines lineage-specific neural progenitor proliferation patterns. *Dev. Biol.* **376**, 150-162.

Markus, R., Laurinyecz, B., Kurucz, E., Honti, V., Bajusz, I., Sipos, B., Somogyi, K., Kronhamn, J., Hultmark, D. and Ando, I. (2009). Sessile hemocytes as a hematopoietic compartment in Drosophila melanogaster. *Proc. Natl. Acad. Sci. USA* **106**, 4805-4809.

Martinez-Agosto, J. A., Mikkola, H. K. A., Hartenstein, V. and Banerjee, U. (2007). The hematopoietic stem cell and its niche: a comparative view. *Genes Dev.* **21**, 3044-3060.

Mergliano, J. and Minden, J. S. (2003). Caspase-independent cell engulfment mirrors cell death pattern in *Drosophila* embryos. *Development* **130**, 5779-5789.

Milton, C. C., Grusche, F. A., Degoutin, J. L., Yu, E., Dai, Q., Lai, E. C. and Harvey, K. F. (2014). The Hippo pathway regulates hematopoiesis in Drosophila melanogaster. *Curr. Biol.* **24**, 2673-2680.

Minakhina, S., Tan, W. and Steward, R. (2011). JAK/STAT and the GATA factor Pannier control hemocyte maturation and differentiation in Drosophila. *Dev. Biol.* **352**, 308-316.

Mondal, B. C., Mukherjee, T., Mandal, L., Evans, C. J., Sinenko, S. A., Martinez-Agosto, J. A. and Banerjee, U. (2011). Interaction between differentiating cell- and niche-derived signals in hematopoietic progenitor maintenance. *Cell* **147**, 1589-1600.

Mondal, B. C., Shim, J., Evans, C. J. and Banerjee, U. (2014). Pvr expression regulators in equilibrium signal control and maintenance of Drosophila blood progenitors. *Elife* **3**, e03626.

Morin, X., Daneman, R., Zavortink, M. and Chia, W. (2001). A protein trap strategy to detect GFP-tagged proteins expressed from their endogenous loci in Drosophila. *Proc. Natl. Acad. Sci. USA* **98**, 15050-15055.

Morin-Poulard, I., Vincent, A. and Crozatier, M. (2013). The Drosophila JAK-STAT pathway in blood cell formation and immunity. *Jak-Stat.* **2**, e25700.

Nakamura-Ishizu, A., Takizawa, H. and Suda, T. (2014). The analysis, roles and regulation of quiescence in hematopoietic stem cells. *Development* **141**, 4656-4666.

Neufeld, T. P. and Edgar, B. A. (1998). Connections between growth and the cell cycle. *Curr. Opin. Cell Biol.* **10**, 784-790.

Oyallon, J., Vanzo, N., Krzemień, J., Morin-Poulard, I., Vincent, A. and Crozatier, M. (2016). Two independent functions of collier/early B cell factor in the control of drosophila blood cell homeostasis. *PLoS ONE* **11**, e0148978.

Pauklin, S. and Vallier, L. (2013). The cell-cycle state of stem cells determines cell fate propensity. *Cell* **155**, 135-147.

Price, D. M., Jin, Z., Rabinovitch, S. and Campbell, S. D. (2002). Ectopic expression of the Drosophila Cdk1 inhibitory kinases, Wee1 and Myt1, interferes with the second mitotic wave and disrupts pattern formation during eye development. *Genetics* **161**, 721-731.

Rizki, T. M. and Rizki, R. M. (1992). Lamellocyte differentiation in Drosophila larvae parasitized by Leptopilina. *Dev. Comp. Immunol.* **16**, 103-110.

Russell, P. and Nurse, P. (1986). cdc25+ functions as an inducer in the mitotic control of fission yeast. *Cell* **45**, 145-153.

Russell, P. and Nurse, P. (1987). Negative regulation of mitosis by wee1+, a gene encoding a protein kinase homolog. *Cell* **49**, 559-567.

Sela, Y., Molotski, N., Golan, S., Itskovitz-Eldor, J. and Soen, Y. (2012). Human embryonic stem cells exhibit increased propensity to differentiate during the G1

Development (2017) 144, 2415-2427 doi:10.1242/dev.149641

phase prior to phosphorylation of retinoblastoma protein. *Stem Cells* **30**, 1097-1108.

Shim, J., Gururaja-Rao, S. and Banerjee, U. (2013). Nutritional regulation of stem and progenitor cells in Drosophila. *Development* **140**, 4647-4656.

Sinenko, S. A., Mandal, L., Martinez-Agosto, J. A. and Banerjee, U. (2009). Dual role of wingless signaling in stem-like hematopoietic precursor maintenance in Drosophila. *Dev. Cell* **16**, 756-763.

Singh, A. M., Sun, Y., Li, L., Zhang, W., Wu, T., Zhao, S., Qin, Z. and Dalton, S. (2015). Cell-cycle control of bivalent epigenetic domains regulates the exit from pluripotency. *Stem Cell Rep.* **5**, 323-336.

Small, C., Paddibhatla, I., Rajwani, R. and Govind, S. (2012). An introduction to parasitic wasps of Drosophila and the antiparasite immune response. *J. Vis. Exp.* e3347.

Small, C., Ramroop, J., Otazo, M., Huang, L. H., Saleque, S. and Govind, S. (2014). An unexpected link between notch signaling and ROS in restricting the differentiation of hematopoietic progenitors in Drosophila. *Genetics* **197**, 471-483.

Stevens, A. and Jacobs, J. R. (2002). Integrins regulate responsiveness to slit repellent signals. *J. Neuro.* **22**, 4448-4455.

Stramer, B., Wood, W., Galko, M. J., Redd, M. J., Jacinto, A., Parkhurst, S. M. and Martin, P. (2005). Live imaging of wound inflammation in Drosophila embryos reveals key roles for small GTPases during in vivo cell migration. *J. Cell Biol.* **168**, 567-573.

Tan, K. L., Goh, S. C. and Minakhina, S. (2012). Genetic screen for regulators of lymph gland homeostasis and hemocyte maturation in Drosophila. *G3* **2**, 393-405.

Tapias, A., Zhou, Z.-W., Shi, Y., Chong, Z., Wang, P., Groth, M., Platzer, M., Huttner, W., Herceg, Z., Yang, Y.-G. et al. (2014). Trrap-dependent histone acetylation specifically regulates cell-cycle gene transcription to control neural progenitor fate decisions. *Cell Stem Cell* **14**, 632-643.

Tokusumi, T., Shoue, D. A., Tokusumi, Y., Stoller, J. R. and Schulz, R. A. (2009). New hemocyte-specific enhancer-reporter transgenes for the analysis of hematopoiesis in Drosophila. *Genesis* **47**, 771-774.

Xu, T. and Rubin, G. M. (1993). Analysis of genetic mosaics in developing and adult Drosophila tissues. *Development* **117**, 1223-1237.

Zhang, L., Tran, D. T. and Ten Hagen, K. G. (2010). An O-glycosyltransferase promotes cell adhesion during development by influencing secretion of an extracellular matrix integrin ligand. *J. Biol. Chem.* **285**, 19491-19501.

Zhang, C. U., Blauwkamp, T. A., Burby, P. E. and Cadigan, K. M. (2014). Wnt-mediated repression via bipartite DNA recognition by TCF in the Drosophila hematopoietic system. *PLoS Genet.* **10**, e1004509.

Zhou, G.-Q., Zhang, Y., Ferguson, D. J. P., Chen, S., Rasmuson-Lestander, A., Campbell, F. C. and Watt, S. M. (2006). The Drosophila ortholog of the endolysosomal membrane protein, endolyn, regulates cell proliferation. *J. Cell. Biochem.* **99**, 1380-1396.

SUPPLEMENTAL MATERIALS AND METHODS

Drosophila stocks

All *Drosophila melanogaster* stocks were maintained on standard yeast extract/glucose media. For UAS-Tig transgenics, expression strength of multiple transgenic lines were compared by immunostaining with *Hemolectin*-Gal4 (*Hml*-Gal4), comparing signal intensities using imageJ.

Immunohistochemistry and in situ hybridization

For secondary antibodies used in immunostainings, donkey anti-mouse/rabbit IgG, Cy5/Cy3 (Jackson ImmunoResearch Laboratories Inc., 715-165-151, 715-175-171, 111-165-144 & 111-175-144) and A488 (Thermo Fisher Scientific, A11001 & 11034) were used at 1:300 and 1:1000, respectively.

Imaginal discs were dissected, fixed and mounted and their area determined by ImageJ. The relative number of circulating hemocytes were determined essentially as described (Zettervall et al., 2004). In brief, wandering third instar larva were washed in PBS and then placed in a microtiter well with 30µl PBS. The body wall of each larvae were ripped apart with fine forceps and the carcass washed with a fine pipet tip. Three samples/larvae were counted with a hemocytometer. Six biological replicates were determined for each condition and the data expressed as the mean $\pm$ s.d.

For in situ detection of Tig mRNA, hybridization of larval PLs was performed as according to a published protocol (Iwasaki et al., 2013). Samples were photographed with DIC optics using a Leica DM6000 B upright microscope system, taking optical slices. The MZ and CZ were identified by cellular morphology as described previously (Jung et al., 2005), with the CZ containing larger more loosely packed cells forming a grainy surface, while the MZ had smaller, densely packed cells with smooth surface. The PLs were photographed in both DIC and brightfield optics and the DIC images were used to delineate the MZ/CZ border, while the brightfield images shown in the figure allow for a better comparison of signal strength in the tissue.

To measure the S-index of PLs, larvae were dissected within 30 min before being

labeled in 10 µM EdU (diluted in PBS) for 70 min, then washed 2 x 5 min in PBS and fixed in 4% formaldehyde. If combined with immunostaining, blocking, primary and secondary antibodies were added, after which EdU was visualized by the Click-iT EdU Alexa Fluor 555 Imaging Kit (Life Technologies). Samples were then washed 2 x 5 min in PBST (PBS + 0.5% Triton-X100), stained with DAPI for 30 min, washed 4 x 5 min in PBST, and mounted in Vectashield. The M-index was determined by immunostaining for histone H3 (phosphor S10 with pH3 antibody (Millipore). S-index was quantified using images taken approximately one-third from the top of the PL. Due to their lower occurrence, M-phase cells were counted from projected stacks of PLs.

Imaging and Data Quantification

For samples marked with P1, Hml>GFP and DAPI, PL was determined by DAPI, CZ by Hml>GFP, IP by GFP^+ $P1^-$, and MZ by $DAPI^+$ GFP^-. For samples marked with Hml and Dome reporters, CZ was determined by Hml-dsRed, MZ by Dome-EBFP, IP by $dsRed^+$ $EBFP^+$, and PL by the total. For crystal cell number, full PL projections were used to count Lz^+ cells. For PSC cell number, the dense packing of the cells made counting difficult. Therefore, full stack projections of Hh>EGFP were used to determine (a) total GFP intensity and (b) average single cell GFP intensity (which was statistically the same between WT and $Tig^{A1/X}$), and PSC cell number was calculated as a/b. There was no significant difference in single cell GFP intensity between control and *Tig* mutant PSCs.

SUPPLEMENTAL REFERENCES

Iwasaki, K., Taguchi, M., Bonkowsky, J. L. and Kuwada, J. Y. (2013). Expression of arginine vasotocin receptors in the developing zebrafish CNS. *Gene Expr. Patterns* **12**, 335-342.

Zettervall, C. J. Anderl, I., Williams, M. J., Palmer, R., Kurucz, E., Ando, I. and Hultmark, D. (2004). A directed screen for genes involved in Drosophila blood cell activation. *Proc. Natl. Acad. Sci. USA* **101**, 14192-14197.

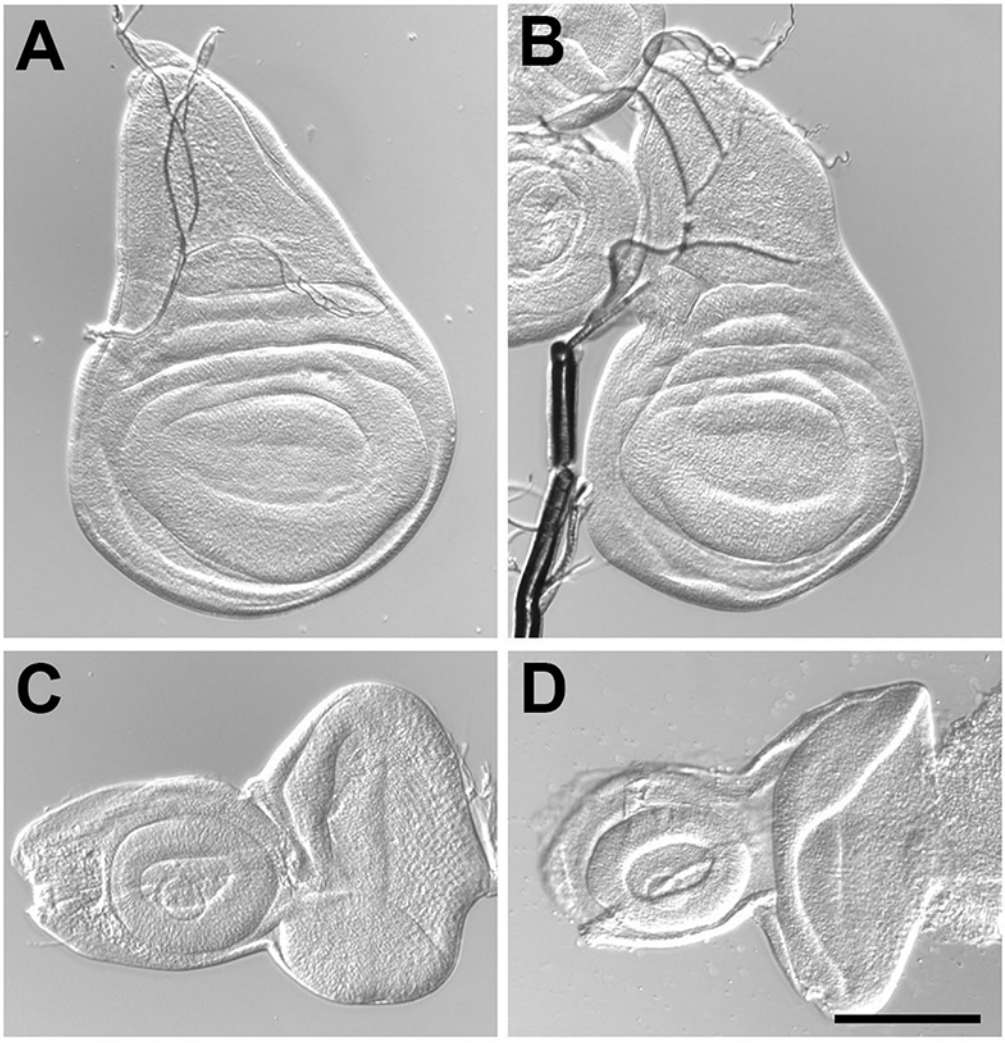

	Mean + SD (n)		
Genotype	Wing disc	Larval eye	Eye/Antennal disc
Wild type	14.0 ± 3.5 (16)	7.6 ± 1.4 (10)	12.8 ± 2.1 (8)
$Tig^{A1/X}$	11.2 ± 2.9 (18)	6.2 ± 1.4 (10)	10.0 ± 1.7 (6)
	P = 0.017	P = 0.034	P = 0.022

Figure S1. Imaginal discs are slightly reduced in size in *Tig* mutants. (A-D) DIC images of wing (A-B) and eye/antennal (C-D) imaginal discs from w^{1118} (A,C) and $Tig^{A1/X}$ wandering 3rd instar larva (B,D). (E) Table showing ImageJ quantification of the area of the imaginal discs. There was an approximate 20% decrease in size of the *Tig* mutants that is statistically significant. Bar = 100µm.

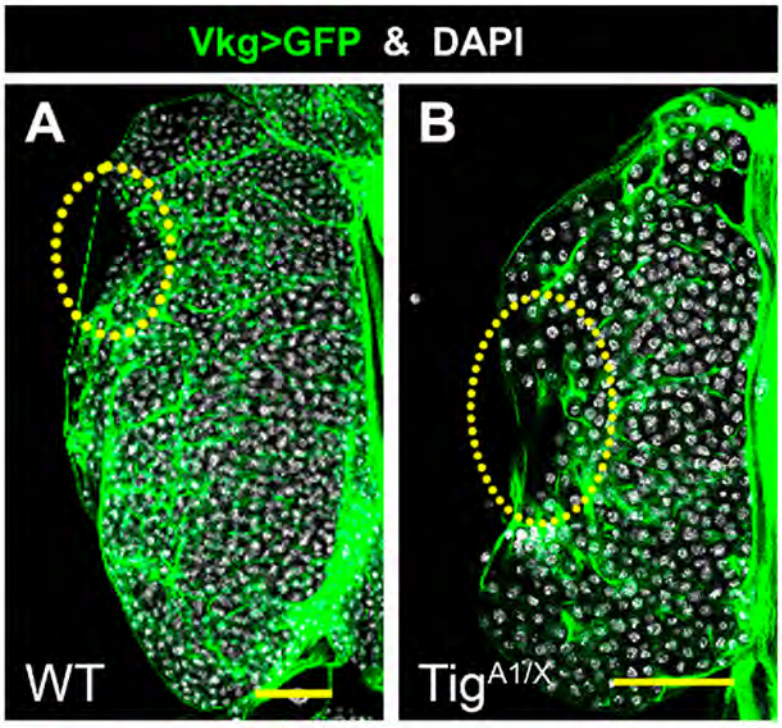

C

Genotype	% of PLs having empty nests (circled in A&B)
WT	27.8% (5/18)
Tig $^{A1/X}$	27.3% (6/22)

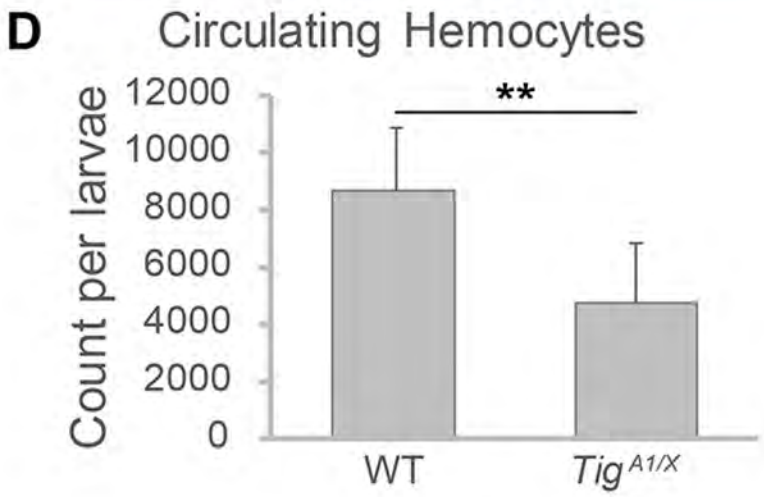

Figure S2. No apparent early release of plasmatocytes from the lymph glands of *Tig* mutants. (A-B) Confocal images of PLs of w^{1118} and $Tig^{A1/X}$ mid/late 3rd instar larva carrying the Vkg-GFP gene trap (green) and stained for DAPI (white). So called "empty nest" areas that contain Vkg-GFP matrix but devoid of cells are indicated (yellow dashed circles). (C) Table indicating no change in the frequency of empty nests in control and *Tig* mutant PLs. (D) Number of circulating hemocytes in control and *Tig* mutants. Hemocytes were collected from the body cavity of mid/late 3rd instar larvae. *Tig* mutants had approximately half the number of circulating hemocytes as wild type. Six animals of each genotype were analyzed and the mean ± s.d. indicated. **: $p<0.01$.

A

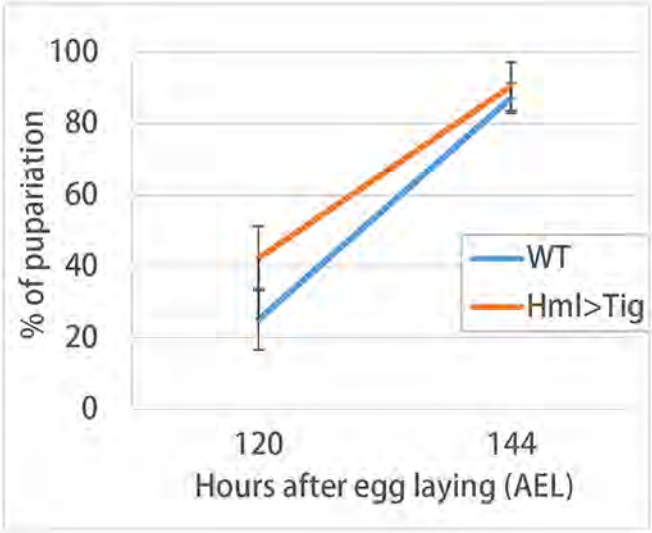

B

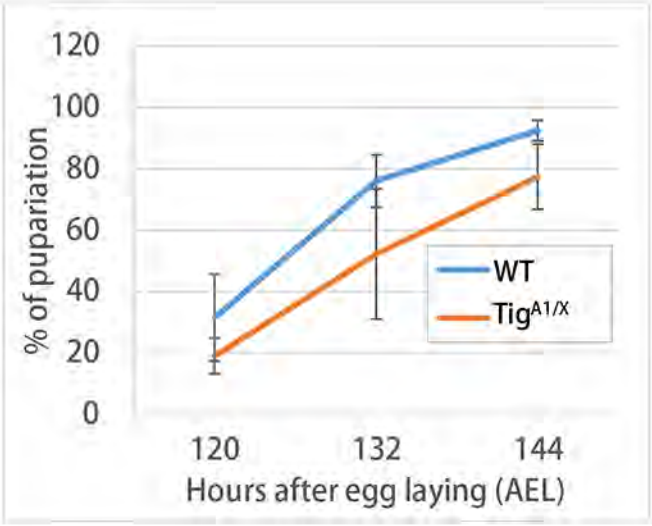

C

Hours AEL	P-value between:	
	WT and $Tig^{A1/X}$	Hml>+ and Hml>Tig
120	0.081	0.037
132	0.066	N.D.
144	0.034	0.259

Figure S3. Developmental kinetics of Hml>Tig and *Tig* mutants. (A-B) Percent of animals reaching pupal stage between w^{1118} controls and Hml>Tig (A) or $Tig^{A1/X}$ (B). Control and Hml>Tig animals developed to pupariation at about the same rate, while *Tig* mutants had a slight (~6-12 hr) delay. (C) Table showing the P-values for each point, which represent a sample size of >150 animals. Animals were reared at 29˚C for panel A and 25˚C for panel B.

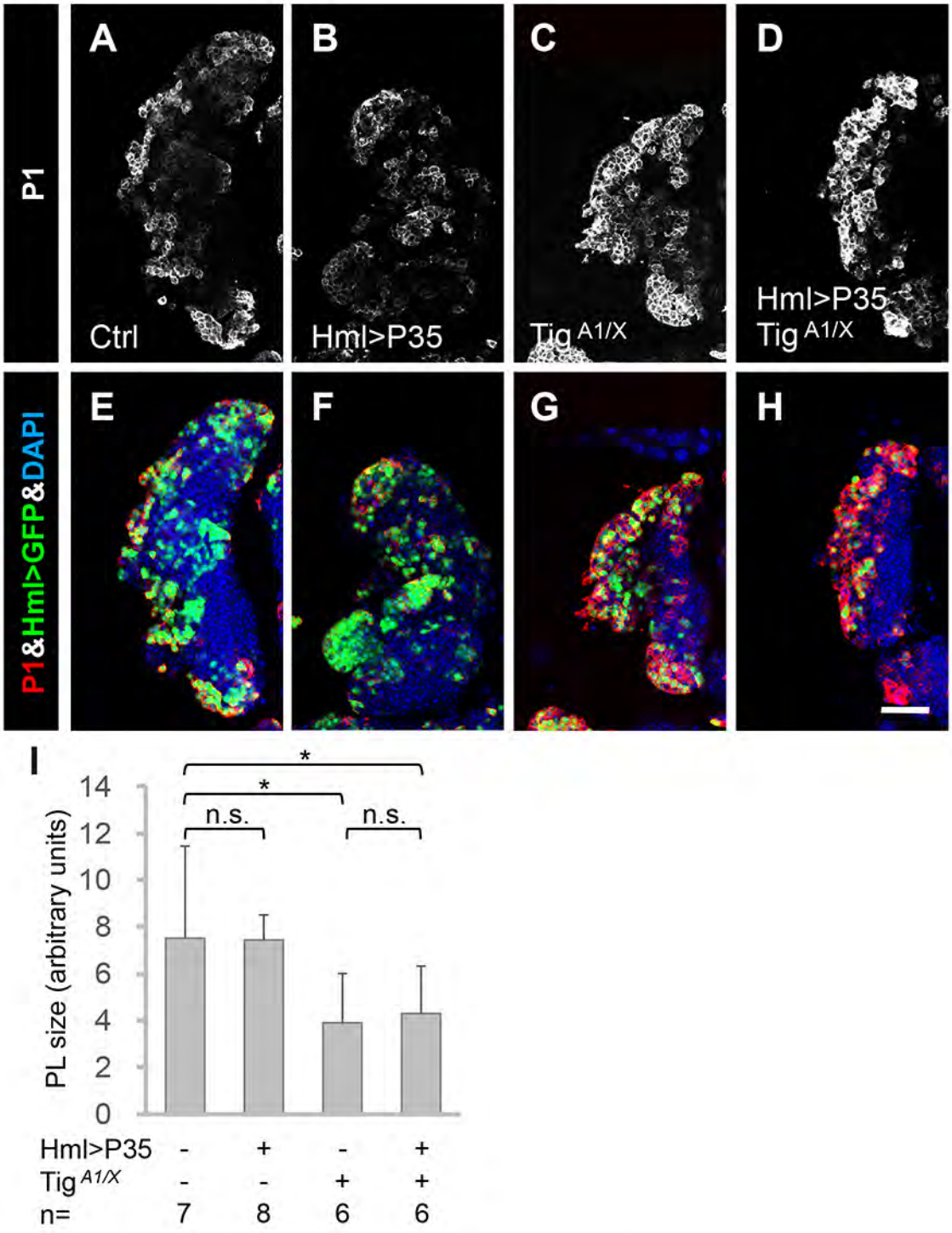

Figure S4. Inhibition of apoptosis does not rescue the *Tig* mutant phenotype in PLs. (A-H) Confocal images of PLs from w^{1118} (A,E), Hml>P35 (B,F), $Tig^{A1/X}$ (C,G) and $Tig^{A1/X}$; Hml>P35 animals stained for P1 (white in panels A-D; red in E-H) and DAPI (blue). Hml-Gal4 backgrounds also contained UAS-GFP (green) to mark the CZ. Expression of the caspase inhibitor P35 via the Hml-Gal4 driver had no detectable rescue of the small PL size and elevated P1 staining in *Tig* mutants. Animals reared at 29˚C. Bar = 50μm.

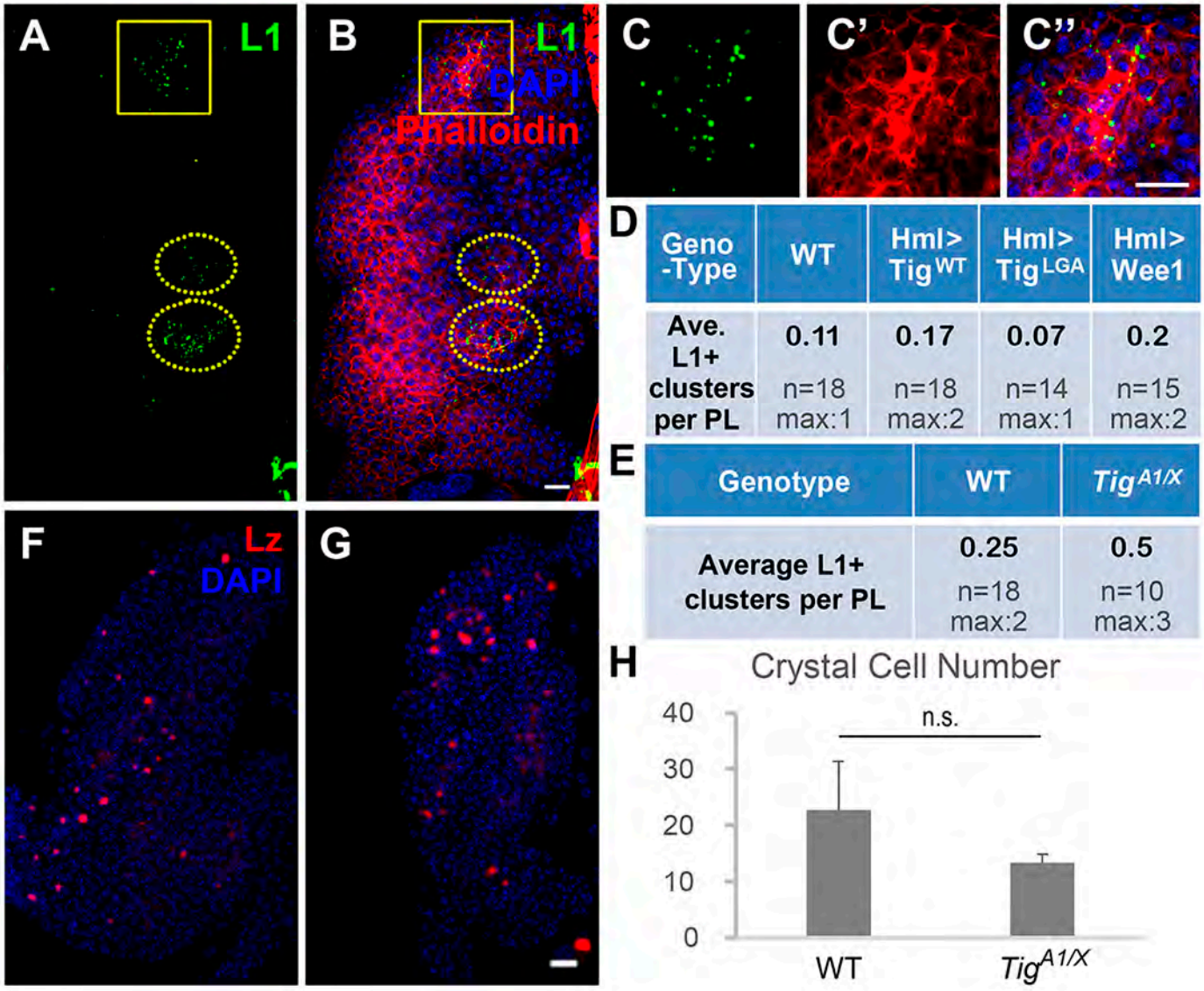

Figure S5. Lamellocyte and Crystal cell fate determination are not affected by Tig and Wee1 manipulation. (A-C'') Confocal images of a PL from mid/late 3rd instar *Tig* mutant larvae stained with the lamellocyte-specific antibody L1 and counterstained with phalloidin. Lamellocytes were identified by punctate L1 signal and verified by a regional increase in phalloidin signal (boxed area magnified in C-C''). While the PL shown contained three lamellocytes, the vast majority of PLs had no lamellocytes. (D-E) Summary of the amount of lamellocyte clusters in Hml>Tig^{WT}, Hml>Tig^{LGA}, Hml>Wee1 and *Tig*$^{A1/X}$ PLs, compared to *w*^{1118} controls. All PLs contained less than one cluster/PL. The distribution of lamellocytes/PL was similar under all experimental conditions. (F-G) Confocal images of PLs from wild-type or *Tig*$^{A1/X}$ mid/late 3rd instar larvae immunostained for Lz. No statistical difference was observed in the number of Lz^{+} cells/PL (n = 6 for each sample). All Hml experiments were performed at 29˚C, while the *Tig* mutants and cognate controls were reared at 25˚C. Bars = 20μm.

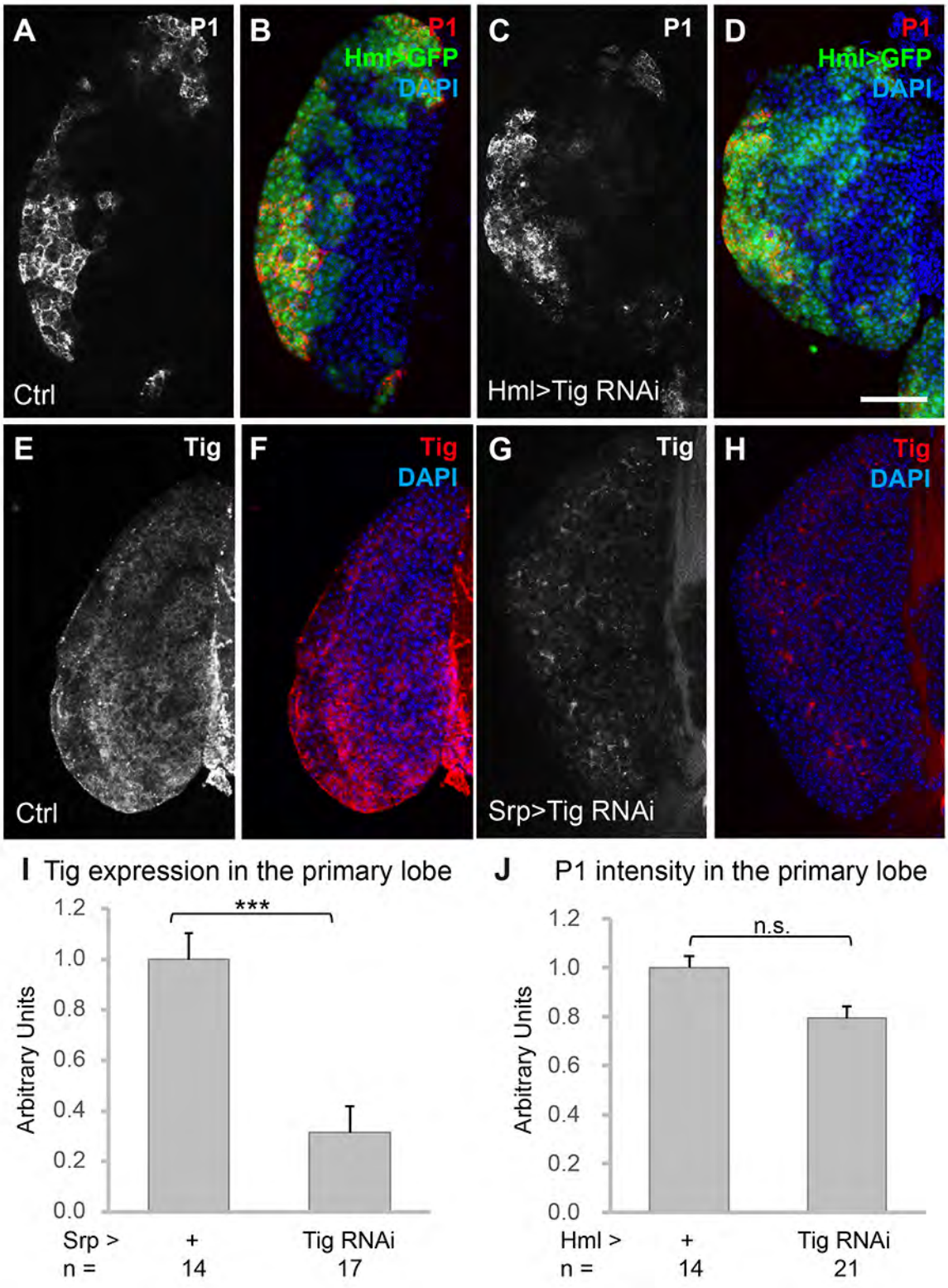

Figure S6. ***Tig*** **RNAi does not change P1 expression in the CZ.** (A,B,E,F) Confocal images of mid/late 3rd instar PLs containing P[Hml-Gal4] and P[UAS-GFP) without (Ctrl) or with P[UAS-TigRNAi] and immunostained for P1. (C,D,G,H) Confocal images of mid/late 3rd instar PLs containing P[Srp-Gal4] without (Ctrl) or with P[UAS-TigRNAi] and immunostained for Tig. Bar = 50 um. (I) Quantification reveals no significant change in the amount of plasmatocytes in Hml>Tig RNAi animals. (J) Quantification shows that Tig protein expression is reduced to ~30% by Tig RNAi. Animals reared at 31 °C. ***: $p<0.001$.

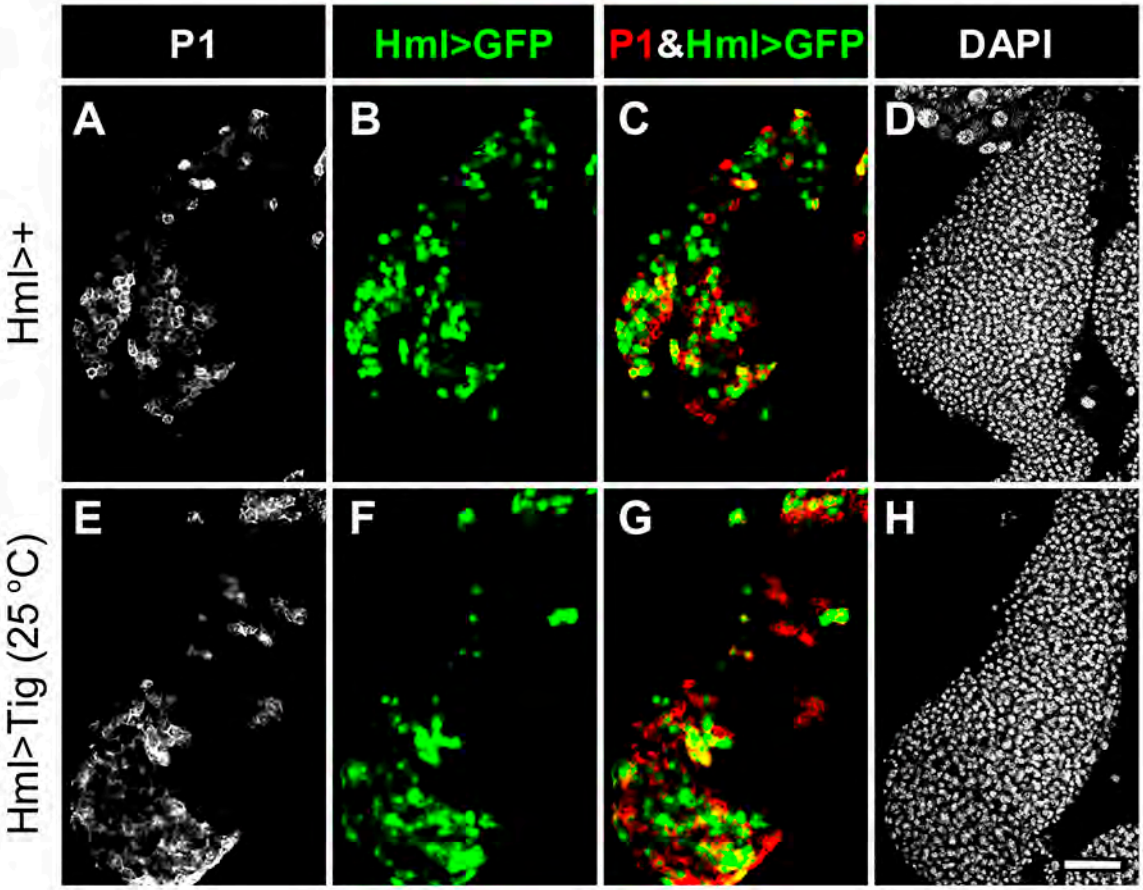

Figure S7. Moderate expression of Tig does not affect plasmatocyte differentiation. Confocal images of mid 3rd instar PLs containing P[Hml-Gal4] and P[UAS-GFP] with or without P[UAS-Tig^{WT}] and immunostained for P1. The amount of plasmatocytes (A,E) and Hml>GFP^{+} cells (B,F) were not detectably affected by Tig overexpression under these conditions (n = 10). Experiments were performed at 25˚C to achieve lower expression than used in Figures 2, 3 & 9. Bar = 50μM.

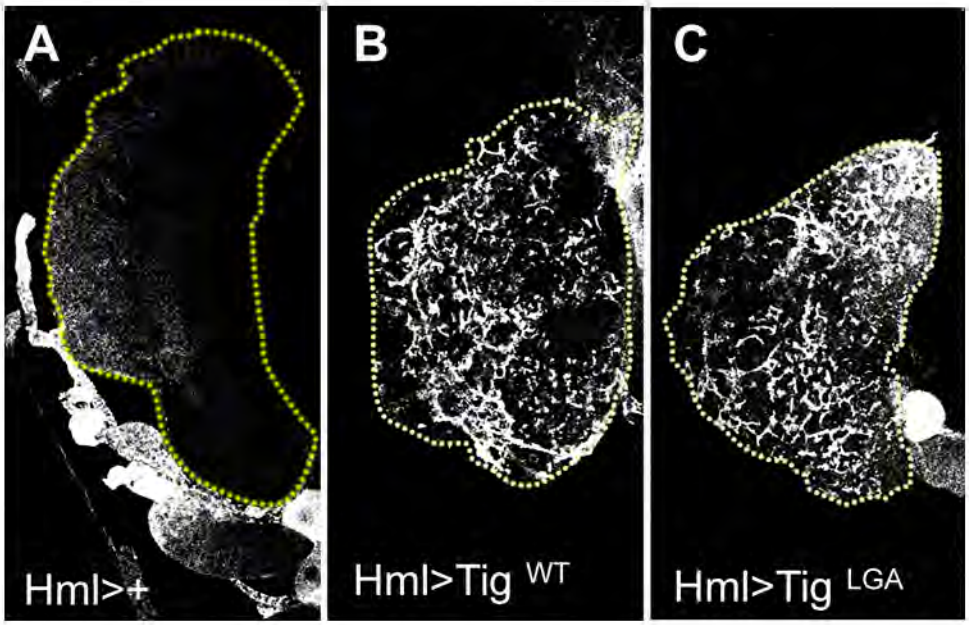

Figure S8. Endogenous Tig is detectable in wild type PLs. (A-C) The same confocal images shown in Fig. 4C, H & M but with increased sensitivity, which oversaturated the Hml>Tig PLs (B-C) but allowed endogenous Tig protein to be observed.

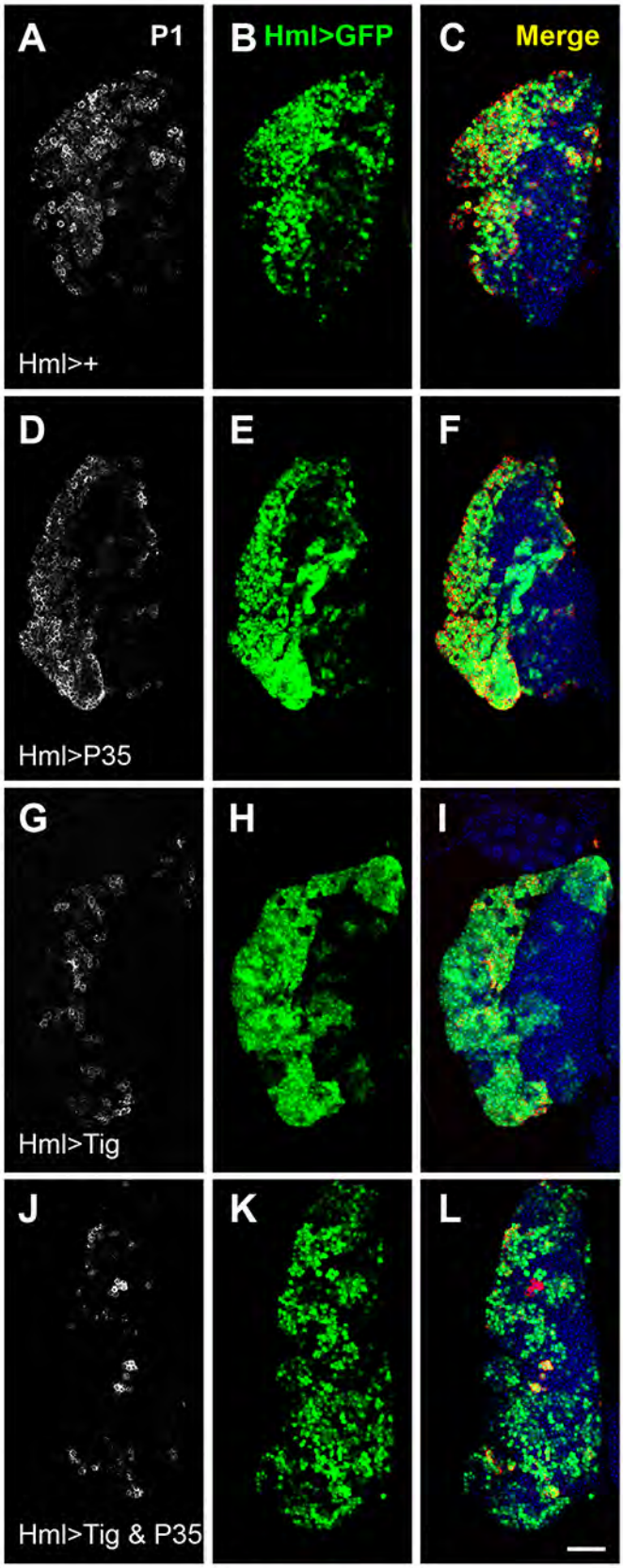

Figure S9. Expression of a caspase inhibitor does not suppress the Hml>Tig phenotype in PLs. (A-L) Confocal images of mid/late 3rd instar PLs containing P[Hml-Gal4] and P[UAS-GFP] (A-C) plus either P[UAS-P35] (D-F), P[UAS-Tig] (G-I) or both (J-L). All PLs were stained with P1 (white) and DAPI (blue) and GFP signal is shown as green. Expression of P35 has no detectable effect on plasmatocyte levels (compare panels A & D) and does not alter the Tig-dependent loss of mature plasmatocytes (panels G & J). Eight PLs were examined for each condition. Animals were reared at 29°C. Bar = 50μM.

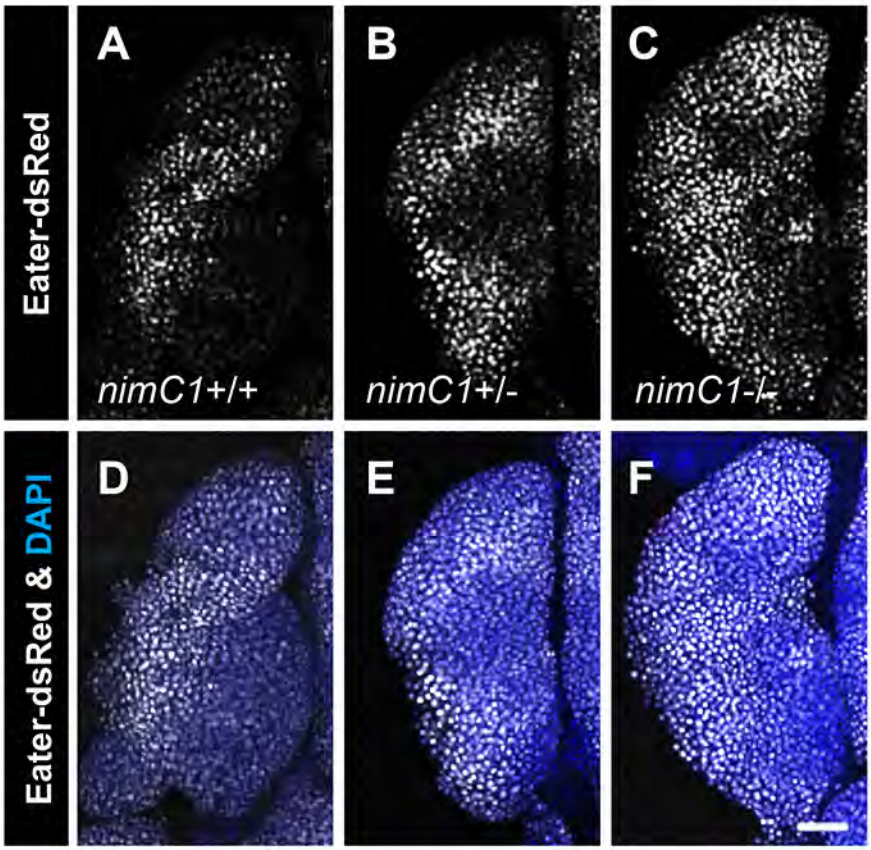

G

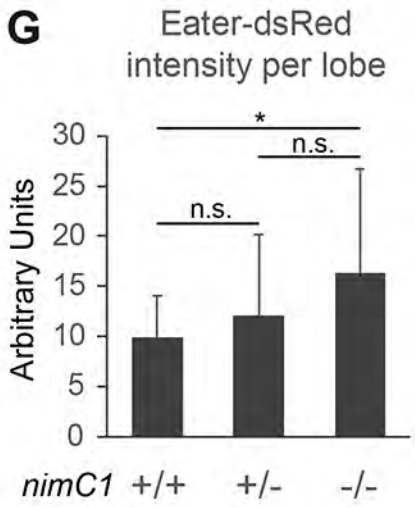

H

Total Eater-dsRed Intensity			
nimC1	WT	het	mut
low	0	2	4
mid	10	9	13
high	1	4	11
Total	11	15	28

Figure S10. Loss of *nimC1* activity does not reduce expression of the Eater-dsRed reporter in PLs. (A-F) Confocal images of PLs from Eater-dsRed animals homozygous for a wild type *nimC1* allele (+/+; A,D), heterozygous for the *nimC1* deletion allele (+/-; B,E) and a *nimC1* homozygous deletion mutant (-/-; C,F). Eater-dsRed (white) and DAPI (blue) signals are shown. Bar = 50μM. (G) Quantification of the Eater-dsRed intensity in each PL showed a small but statistically significant increase in Eater-dsRed in *nimC1* mutants compared to wild type controls. (H) Table grouping PLs of the indicated genotypes as low, mid or high Eater-dsRed staining. While "high" expressers were rare in wild type PLs and *nimC1*/+ heterozygotes, they constituted a sizeable (39%) fraction of *nimC1* mutants.

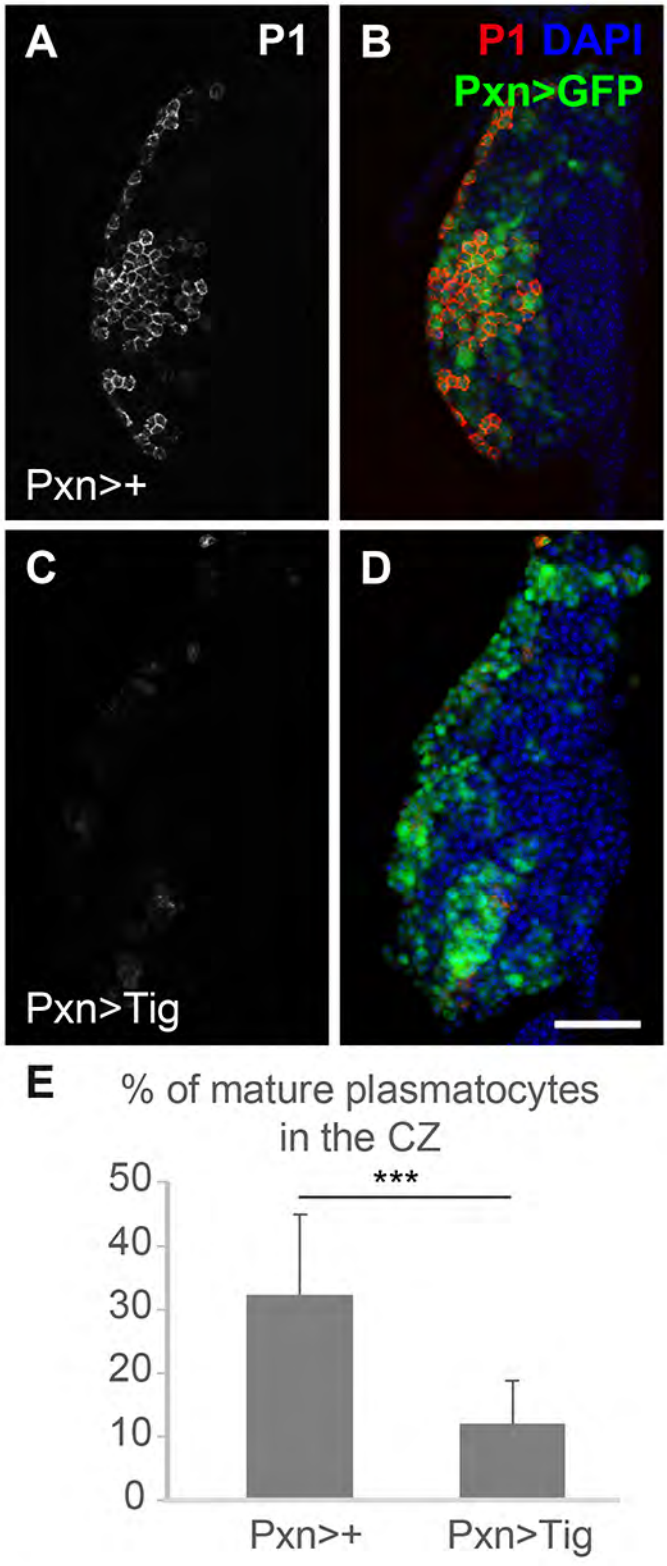

Figure S11. Expression of Tig via the Pxn-Gal4 driver blocks plasmatocyte differentiation. (A-D) Confocal images of of mid/late-3rd instar PLs containing P[Pxn-Gal4] and P[UAS-GFP] alone (A-B) or with P[UAS-Tig] (C-D) stained for P1 (red) and DAPI (blue). GFP signal is in green. Bar = 50µM. (E) Quantification showing a robust reduction of P1^{+} cells in the Pxn>Tig PLs. Animals were reared at 29˚C and 15 PLs were analyzed for each condition. ***: p<0.001.

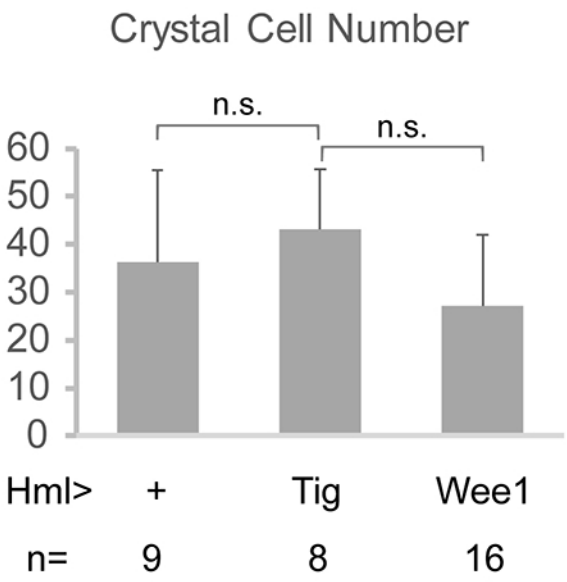

Figure S12. Crystal cell specification is not altered by CZ expression of Tig or Wee1. Bar graph summarizing data from mid/late 3rd instar PLs containing P[Hml-Gal4] plus either P[UAS-Tig] or P[UAS-wee1] immunostained for Lz. No statistically significant difference in crystal cells/PL was detected between the groups.

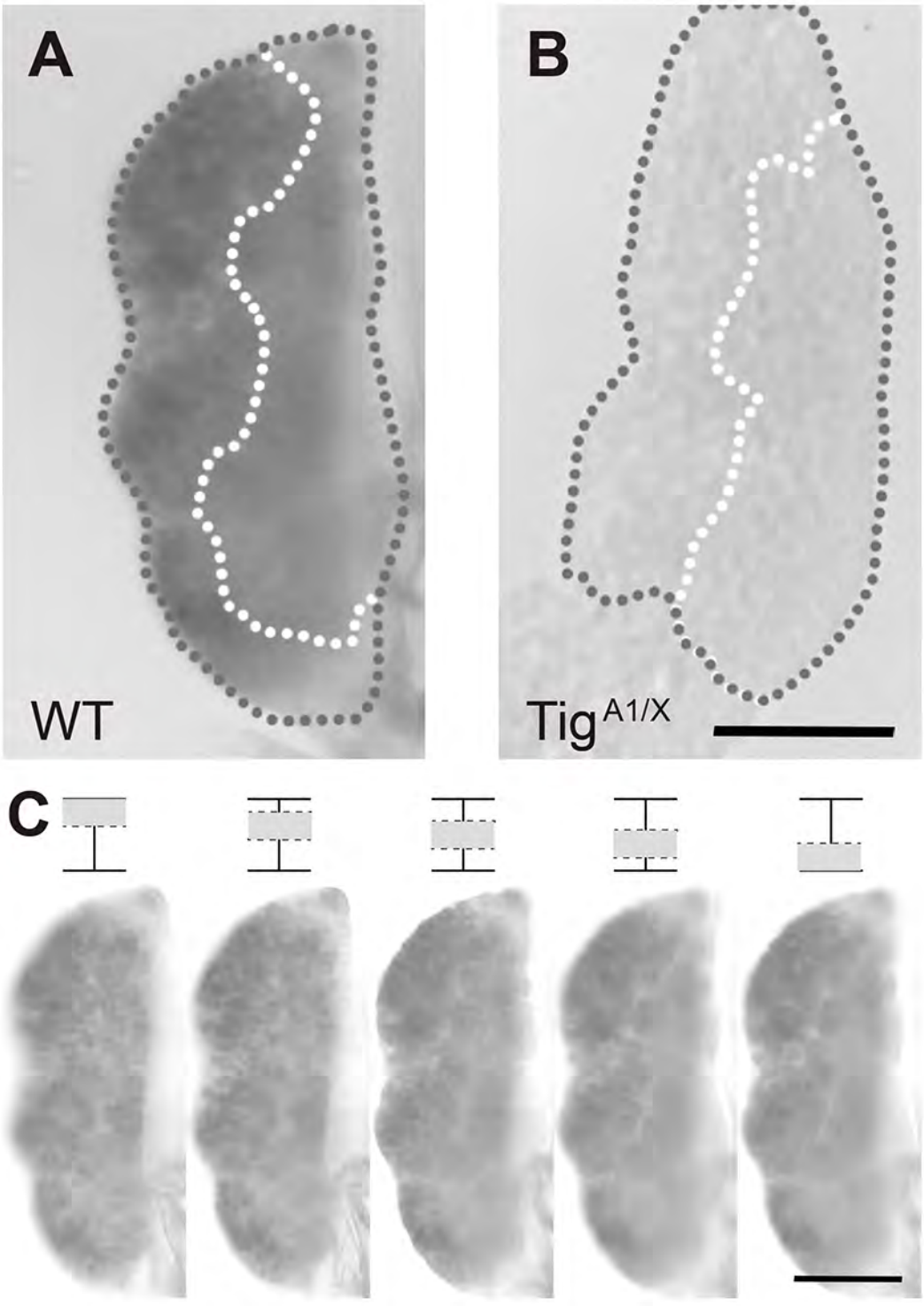

Figure S13. *Tig* mRNA is found in both the MZ and CZ of the PL. (A-B) DIC images of w^{1118} and $Tig^{A1/X}$ mid/late-3rd instar PLs stained with an antisense *Tig* cDNA probe. The MZ/CZ border is indicated by the white dotted lines. The lack of staining in *Tig* mutants indicates that the *Tig* mRNA signal was specific in both the MZ and CZ. (C) Optical slices through different planes of a PL showing strong signal in the peripheral cells and less signal in internal cells. The cartoon above each micrograph indicates the depth of the image. Animals were reared at 25˚C and eight PLs were analyzed for each condition. Bar = 100μM.

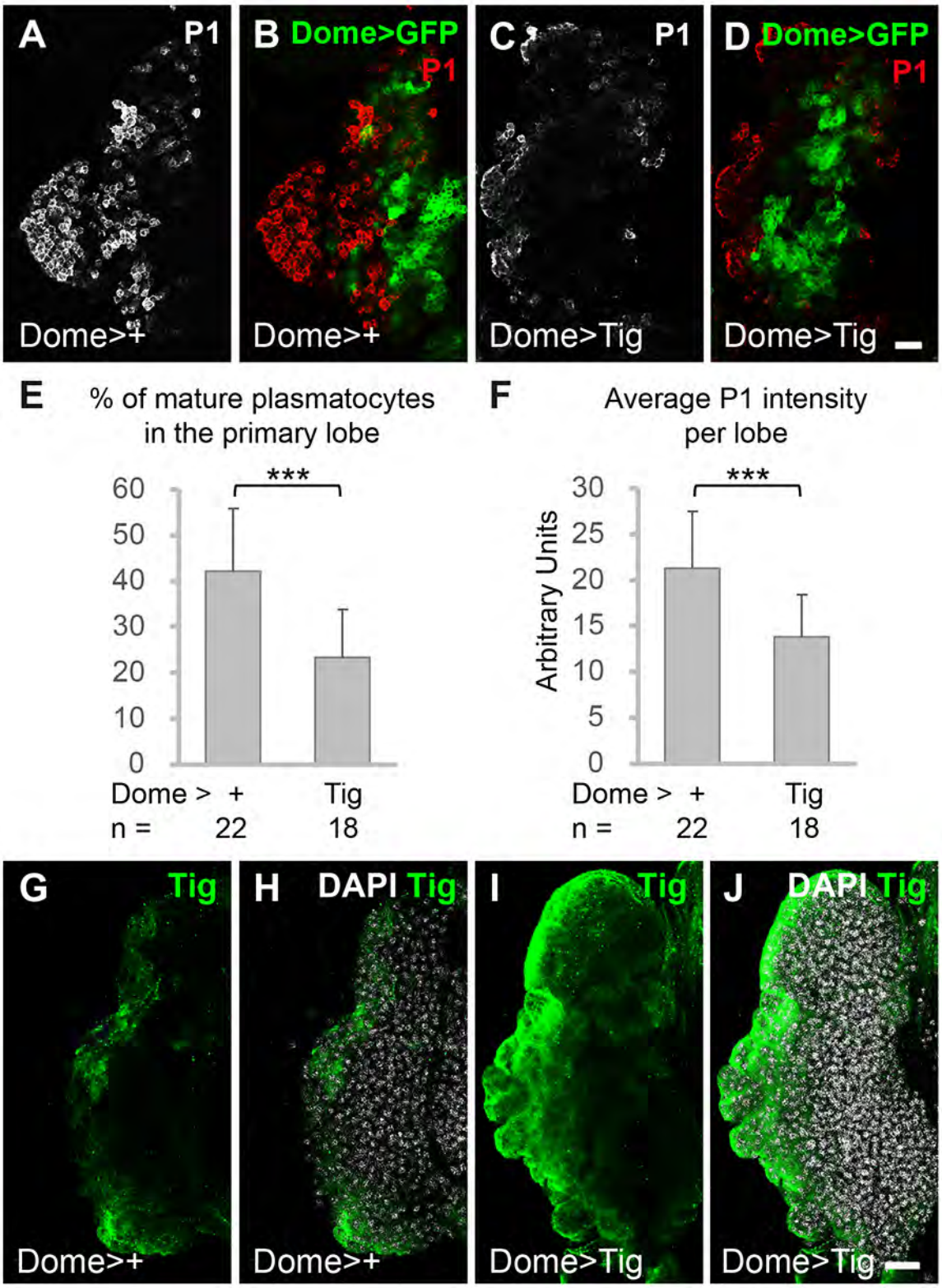

Figure S14. Gal4 driven Tig expression in the MZ results in Tig protein accumulation in the CZ and inhibition of plasmatocytes. (A-D) Confocal images of mid/late 3rd instar PLs containing P[Dome-Gal4] and P[UAS-GFP] (A-B) plus P[UAS-Tig] (C-D) stained with P1 (red). GFP signal is in green. Tig expression dramatically lowered P1 expression in the PL. (E-F) Quantification of P1 staining in the PL, by determining the $P1^{+}$ area/PL (E) or by the average intensity of the P1 signal (F). ***: $p < 0.001$. (G-J) Confocal images of mid/late 3rd instar PLs containing P[Dome-Gal4] and P[UAS-GFP] (G-H) plus P[UAS-Tig] (I-J) stained with Tig (green) and DAPI (white). Despite being transcribed in the MZ, Tig protein accumulated at the periphery of the PL in the CZ. Animals were reared at 29°C. Bars = 50μM.

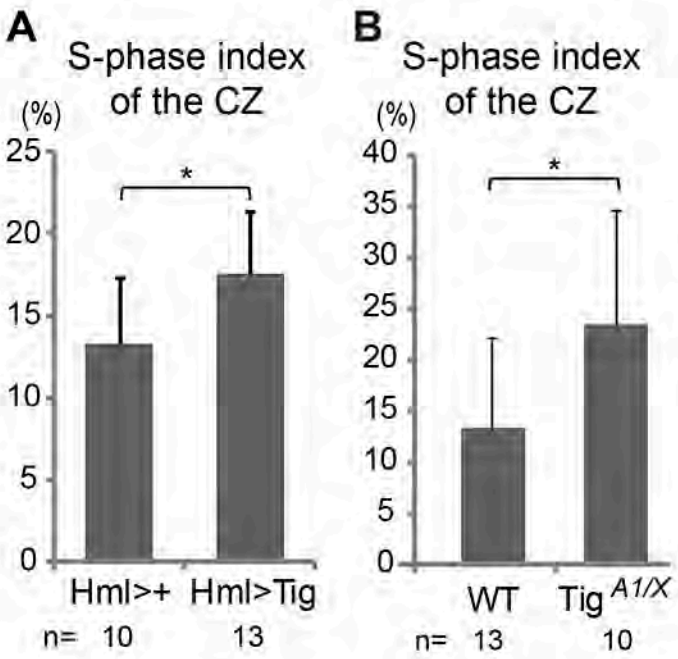

Figure S15. Loss or gain of Tig causes a significant increase in the S-phase index. (A) Quantification of Edu staining of mid/late 3rd instar PLs from P[Hml-Gal4]/+ and P[Hml-Gal4]/P[UAS-Tig] animals reared at 29˚C. (B) Quantification of Edu staining of mid/late 3rd instar PLs from w^{1118} or $Tig^{A1/X}$ mutants reared at 25˚C. *: $p < 0.05$.

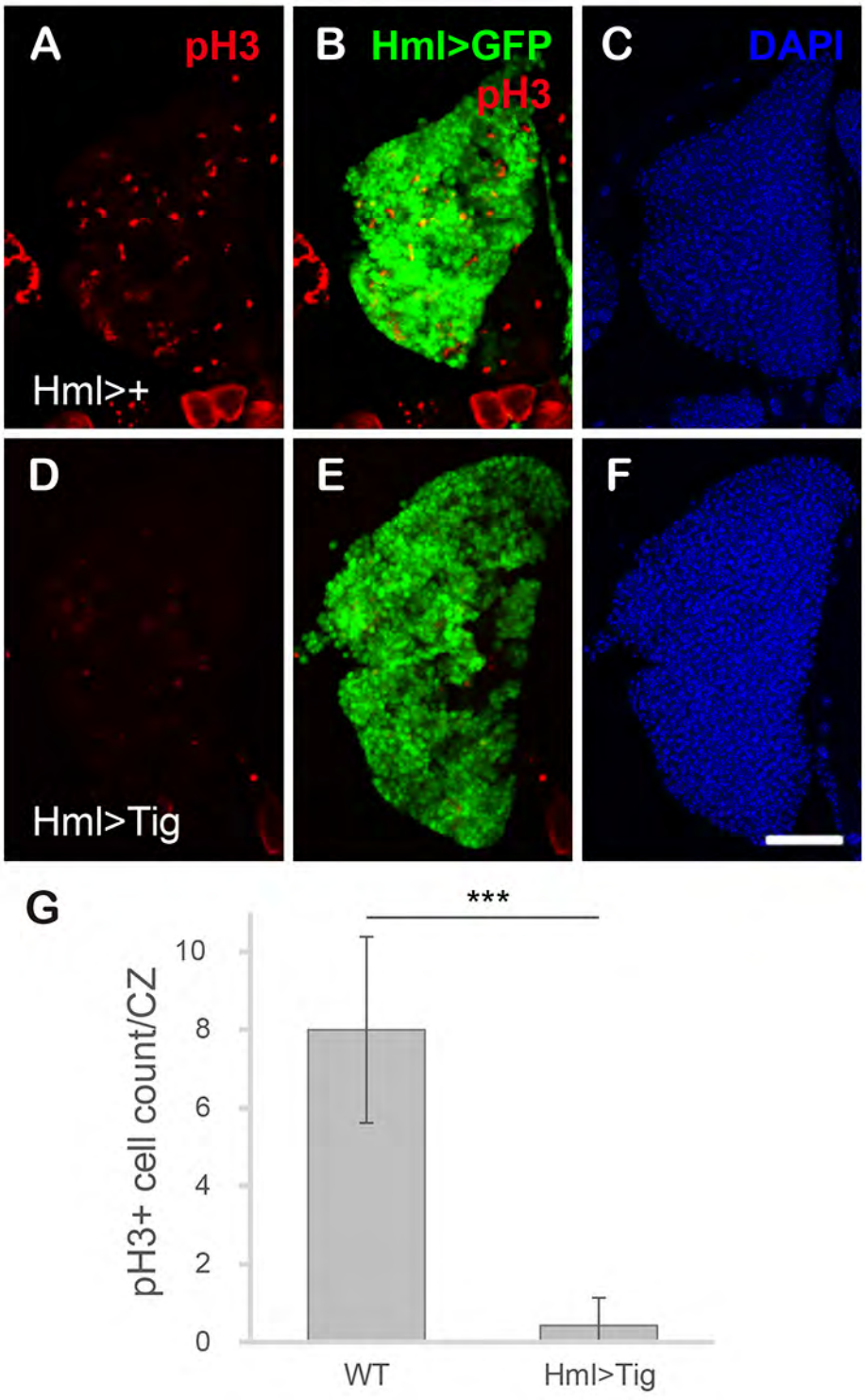

Figure S16. Tig expression in the CZ lowers the mitotic index of the PL. (A-F) Confocal images of mid/late 3rd instar PLs containing P[Hml-Gal4] and P[UAS-GFP] (A-C) plus P[UAS-Tig] (D-F) stained with pH3 antibody (red) and DAPI (blue). GFP signal is in green. Tig expression dramatically lowered pH3 staining throughout the PL. Bar = 50μM. (G) Quantification of the pH3 staining data. Animals were reared at 29°C and 15 PLs were analyzed for each condition. ***: $p < 0.001$.

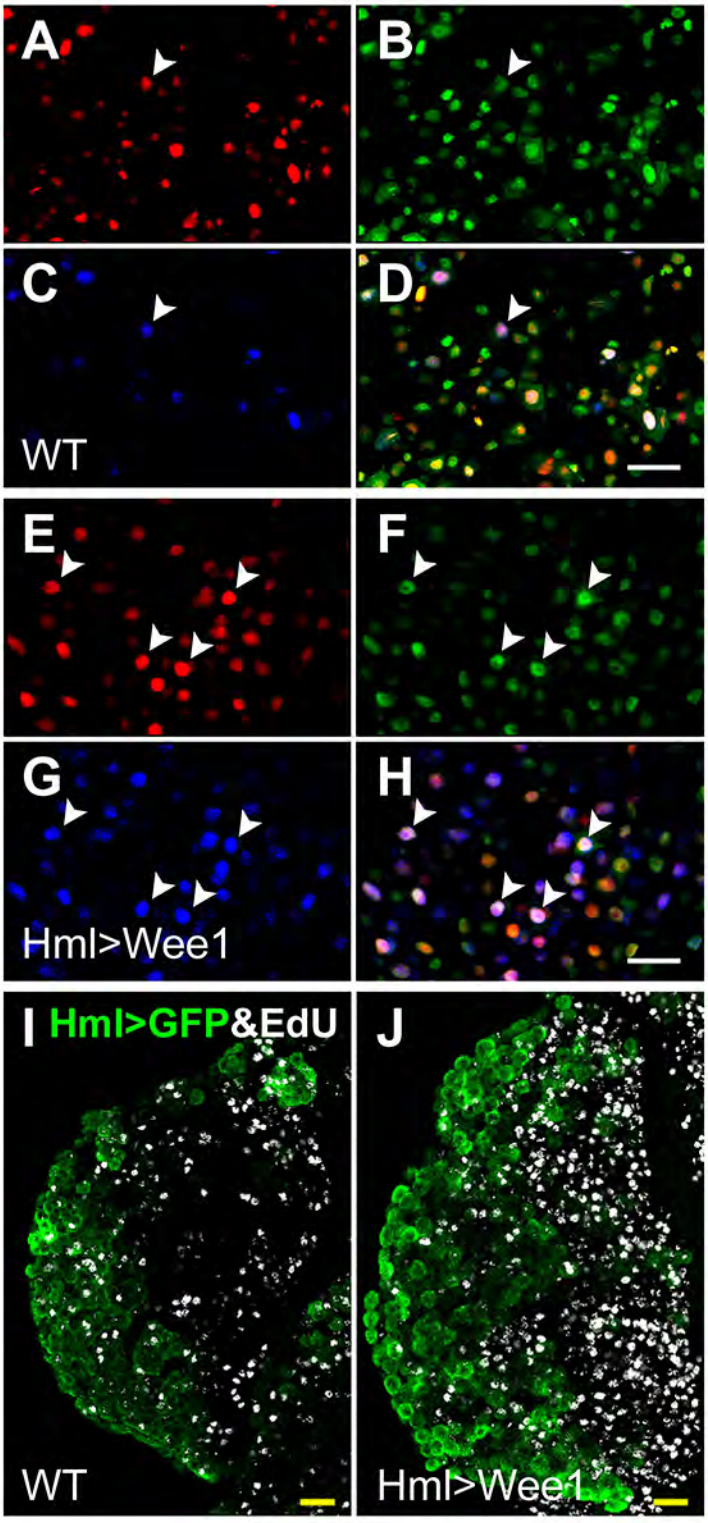

Figure S17. CZ-expression of Wee1 arrests CZ cells at G_2/M transition and induces MZ cell proliferation. (A-L) Confocal images of mid/late 3rd instar LGs containing P[Hml-Gal4] and P[UAS-GFP] with or without P[UAS-Wee1] and labeled with the P[UAS-RGB] cell cycle stage reporter (A-H) or EdU (I-J). The red, green and blue signals are from fluorescent proteins CycB-dsRed, PCNA-GFP and Cdt1- EBFP, respectively. There was an increased number of purple (red^+, $green^+$, $blue^+$) cells in Hml>Wee1 than control LGs (arrowheads in A-H), demonstrating that many cells in Hml>Wee1 were arrested at G_2 (Handke et al., 2014). (I-J) More S-phase cells (EdU^+) were found in the MZ ($Hml>GFP^-$) of Hml>Wee1 LGs. Eight PLs were examined for each condition.

Table S1. Quantification of PL size and percentage of plasmatocytes/PLs using optical slices or entire stacks (volumetric). Both methods gave similar results showing that *Tig* mutant PLs were smaller and have more plasmatocytes/PL.

Stage (larval instar)	Genotype	N	PL size (arb units) (mean ± s.d.)	P value	CZ size (arb units) (mean ± SD)	P value	plasmatocytes/ PL(%) (mean ± s.d.)	P value
late 2nd	w^{1118}	11	33 ± 6.2		15 ± 5.9		8.1 ± 6.5	
late 2nd	$Tig^{A1/X}$	8	30 ± 5.7	0.14	22 ± 5.2	0.0099	14 ± 9.9	0.062
early 3rd	w^{1118}	13	78 ± 20		45 ± 15		24 ± 8.4	
early 3rd	$Tig^{A1/X}$	18	38 ± 21	5.30E-06	29 ± 21	0.014	34 ± 18	0.034
mid/late 3rd	w^{1118}	10	100 ± 28		56 ± 25		26 ± 8.0	
mid/late 3rd	$Tig^{A1/X}$	12	32 ± 14	1.70E-07	28 ± 12	0.0012	50 ± 30	0.011

Table S2. Quantification of data from Figure 2G-I.

Genotype	Method of quantification	N	PL size (arb units) (mean ± SD)	P value	plasmatocytes/PL(%) (mean ± SD)	P value
w^{1118}	optical slice	13	100 ± 20		11 ± 4.1	
$Tig^{A1/X}$	optical slice	24	60 ± 26	1.00E-05	28 ± 7.0	1.00E-09
w^{1118}	volumetric	13	100 ± 26		19 ± 6.1	
$Tig^{A1/X}$	volumetric	24	54 ± 31	8.10E-06	33 ± 13	2.80E-04

Table S3. Quantification of data from Figure 2J-M.

Genotype	MZ-like	CZ-like
w^{1118}	20	2
$Tig^{A1/X}$	6	18

Table S4. Quantification of plasmatocytes/PLs using optical slices or entire stacks (volumetric). Both methods gave similar results showing that expression of Tig or Wee1 via Hml-Gal4 significantly reduced plasmatocytes/PL.

Genotype	Method of quantification	N	plasmatocytes/PL(%) (mean ± SD)	P value
Hml>+	optical slice	15	35 ± 13	
Hml>Tig	optical slice	17	13 ± 9	3.60E-06
Hml>+	volumetric	15	37 ± 10	
Hml>Tig	volumetric	17	14 ± 9	5.00E-08
Hml>+	optical slice	11	38 ± 15	
Hml>Wee1	optical slice	14	15 ± 8	2.00E-05
Hml>+	volumetric	18	27 ± 8	
Hml>Wee1	volumetric	12	18 ± 9	1.00E-03

Table S5. Further quantification of data from Fig. 6, panels A-C & G-I. MZ was defined by Dome-EBFP and CZ by Hml-dsRed. Areas positive for both markers were designated as IP. The MZ and CZ comprised most of the PL with a smaller IP zone. The entire PLs were 18.2% and 37.1% positive for minR-LacZ and Tig-LacZ, respectively. For both reporters, the majority of their expression was in the CZ. When normalized for zone size, minR-LacZ displayed a preference (2.4 fold) for IP and CZ over MZ. In the case of Tig-LacZ, expression was enriched 3.3-fold in IP and 6.1-fold in CZ over the MZ. All quantification was performed on optical slices of 22 PLs for minR-LacZ and 18 PLs for Tig-LacZ.

PL zone	% of total PL	% of minR	%minR/zone
MZ	47.9	29.7	10
IP	8.3	11	24.1
CZ	43.8	59.3	24.7

PL zone	% of total PL	% of Tig1	%Tig1/zone
MZ	49.6	18.3	12.5
IP	13.6	9.2	41.6
CZ	36.7	72.5	76.3